MicroRNA-21 Regulates Metabolic Adaptation of Pathogenic T_H17 cells and Controls Autoimmune Inflammation

Authors

Xiang Yu[1, *], Li Wang[1, *], Chao Yao[2], Rong Qiu[2], Yangge Cui[2], Dai Dai[3], Jun Deng[3], Guojun Hou[2], Yan Wang[2], Jie Qian[1], Yangye Ou[1], Yuting Qin[3], Haibo Zhou[3], Youcun Qian[2], Yuanjia Tang[1], Nan Shen[1,2,3,4]

Affiliations

[1] Shanghai Institute of Rheumatology, Renji Hospital, Shanghai Jiao Tong University School of Medicine, Shanghai, China.
[2] Institute of Health Sciences, Shanghai Jiao Tong University School of Medicine and Shanghai Institutes for Biological Sciences (SIBS), University of Chinese Academy of Sciences, Chinese Academy of Sciences (CAS), Shanghai, China.
[3] China-Australia Centre for Personalized Immunology, Renji Hospital, Shanghai Jiao Tong University School of Medicine, Shanghai, China.
[4] Center for Autoimmune Genomics and Etiology (CAGE), Cincinnati Children's Hospital Medical Center, Cincinnati, Ohio, USA.
Correspondence to Nan Shen, MD, Department of Rheumatology, Renji Hospital, Shanghai Jiao Tong University School of Medicine, 145 Shan Dong Road (c), Shanghai 200001, China. E-mail: nanshensibs@gmail.com.
* These authors contributed equally to the work.

Abstract

T_H17 cells exhibit great heterogeneity and variable functional states in vivo. However, the precise molecular mechanism for this heterogeneity is poorly understood. Here we demonstrate that homeostatic and pathogenic T_H17 cells in vivo show discrete chromatin states at conserved regulatory region of T_H17 cell-related transcription factors, metabolic regulators and microRNAs. We find the regulatory region of *miR-21* shows great more chromatin accessibility in

CNS infiltrating pathogenic T_H17 cells compared to ileum homeostatic T_H17 cells. We further demonstrate that homeostatic and pathogenic T_H17 cells have distinct metabolic states, and miR-21 is essential for the highly glycolytic state of pathogenic T_H17 cells. *MiR-21*-deficient T_H17 cells show less glycolytic activity and express less pathogenic T_H17 cell signature genes. These findings suggest that miR-21 is a critical regulator for the metabolic adaptation of pathogenic T_H17 cells under autoimmune inflammation.

Introduction

T_H17 cells, which have been characterized as a subset of effector $CD4^+$ helper T cells that produce IL-17A[1]. Depending on the sites where they are found, they can be divided into two groups: IL10-producing non-pathogenic T_H17 cells and IFNγ or GM-CSF-producing pathogenic T_H17 cells[2]. Under steady state condition, T_H17 cells producing IL-10 are mainly found at sites of intestinal lamina propria (ileum T_H17 cells), where they mediate mucosal defense[3, 4]. Under inflammatory condition, T_H17 cells acquire the capability to produce IFNγ or GM-CSF (EAE CNS infiltrating, *Citro Rodentium*-induced colon T_H17 cells), and are often seen at sites of inflammatory loci[5, 6]. T_H17 cells also could be differentiated in vitro by a combination of cytokines TGF-β1, IL-6 or IL-6, IL-1β and IL-23[7, 8]. However, the inner differences of these in vivo and in vitro-derived T_H17 cells were not well studied.

It remains unclear what makes a T_H17 cell pathogenic. Studies have shown that T_H17 cells can selectively produce IL-10 or IFNγ when mice are infected with

different pathogens, and IL-1R signaling is essential for the induction of IFNγ while suppressing of IL-10[6]. The cytokine GM-CSF also is reported to be critical for the pathogenesis of T_H17 cells[9, 10]. Recently it is reported that environmental factors such as salt can function to promote pathogenic T_H17 cells development in vivo. Sodium chloride induced Sgk1 is essential for the maintenance of pathogenic T_H17 cells[11, 12]. And by single cell RNA-seq of both in vitro and in vivo-derived T_H17 cells, CD5L was identified as a potential negative regulator of the pathogenicity of T_H17 cells[13, 14].

Upon antigen stimulation, lymphocytes undergo extensive clonal expansion and differentiation for immune defense and regulation. Activated lymphocytes are highly metabolic and demonstrate a striking increase in glycolysis[15, 16, 17]. c-Myc, Hif1a, c-Rel and mTORc1-dependent glycolytic activity is crucial for effective T and B cell immune response[18, 19, 20, 21, 22], whereas Foxo1 and Foxp3 proteins function as key metabolic repressors that contain glycolytic activity in Treg cells[23, 24]. Recently it is reported that by restricting glucose availability, tumor cells limit aerobic glycolysis and effector function of tumor-infiltrating T cells[25, 26]. So far, the metabolic state of T_H17 cells in vivo under different circumstances is not well studied.

MicroRNAs are a class of noncoding RNAs that modulate gene expression at the posttranscriptional level[27]. Specific microRNAs, such as miR-146a, miR-155, and miR-17-92 cluster, were initially shown to be upregulated during the

macrophage inflammatory response. Mice deficient of miR-146a had severe multiple organ autoimmune disease[28]. And miR-155 knockout mice had reduced germinal center response under viral infection[29, 30]; however, these mice were highly resistant to develop EAE disease due to defective T_H17 cell differentiation[31, 32, 33]. Recently, miR-183-96-182 cluster was also reported to be critical for T_H17 cell pathogenicity[34]. However, the regulation of T_H17 cell adaptation in vivo to different microenvironment (homeostatic, autoimmune and pathogen infection) by microRNAs is not well understood.

Recently, ATAC-seq (Assay for transposase-accessible chromatin) technology was developed to study global chromatin changes by using relatively low cell number[35]. It was successfully used to study global chromatin dynamics of Treg cells under inflammatory condition[36], the development of plasmacytoid DC[37] and tumor-specific $CD8^+$ T cells[38]. In this study, by ATAC-seq technology we demonstrate that homeostatic and pathogenic T_H17 cells in vivo have variable chromatin states at the regulatory region of T_H17 cell-related transcription factors, metabolic regulators and microRNAs. The regulatory region of miR-21 shows great more chromatin accessibility in CNS infiltrating pathogenic T_H17 cells. Further study demonstrates that miR-21 is required for the maintenance of pathogenic T_H17 cells in vivo in a T cell-intrinsic manner. Interestingly, we find that homeostatic and pathogenic T_H17 cells have great distinct metabolic states, with pathogenic T_H17 cells highly glycolytic, and miR-21 is essential for the highly glycolytic activity of pathogenic T_H17 cells by targeting the E3

ubiquitin ligase Peli1-c-Rel pathway. These findings suggest that miR-21 is a novel regulator of the metabolic and effector function of pathogenic T_H17 cells.

Results

T_H17 Cells show great discrete chromatin states in vivo

We performed ATAC-seq to assess chromatin states genome-wide of T_H17 cells derived in vivo. We found that non-pathogenic and pathogenic T_H17 cells had discrete chromatin states (Fig. 1a-b). CNS infiltrating pathogenic T_H17 cells showed great differential global chromatin accessibility compared to ileum homeostatic T_H17 cells, whereas the difference between colon *Citro Rodentium* induced T_H17 cells and ileum homeostatic T_H17 cells was much smaller. Principle component analysis of enriched peaks indicated that T_H17 cells in vivo had discrete chromatin states (Fig. 1c), with the major variance came from CNS infiltrating T_H17 cells, chromatin states between ileum homeostatic and *Citro Rodentium* induced colon T_H17 cells were much similar, which indicate that these two types of T_H17 cells may have similar functional property, for mucosal defense against intestinal pathogens. Interestingly, the regulatory region of key T_H17 cell-related transcription factors *Batf* and *Irf4* showed great more chromatin accessibility in pathogenic CNS infiltrating T_H17 cells compared to ileum homeostatic T_H17 cells (Fig. 1d), both Batf and Irf4 were previously shown to be critical for initial activation during T_H17 cell differentiation, whereas the regulatory region of transcription factor c-*Maf* and *Ahr* was with significantly reduced chromatin accessibility in CNS infiltrating pathogenic T_H17 cells, both

c-Maf and Ahr were shown to be repressor of T_H17 cell program. Together, these data suggest that T_H17 cells in vivo have distinct chromatin states.

T_H17 cells also could be differentiated in vitro by a combination of cytokines TGF-β1, IL-6 or IL-6, IL-1β and IL-23, we also analyzed the global chromatin states of these in vitro derived T_H17 cells. We found that pathogenic T_H17 (23) and non-pathogenic T_H17 (b) cells show distinct chromatin states (Supplementary Fig. 1a-b), however, chromatin states of these in vitro derived T_H17 cells could only partially reflect the global chromatin states of their in vivo counterparts.

IL-6 and STAT3-dependent activation of miR-21 in pathogenic T_H17 cells

Interestingly, we found that the regulatory region of certain microRNAs also showed great more chromatin accessibility in CNS infiltrating pathogenic T_H17 cells compared to ileum homeostatic T_H17 cells, which include *miR-21a, miR-23a cluster,* and *miR-210* (Fig. 2a-b), whereas the regulatory region of *miR-125a* cluster was with significantly reduced chromatin accessibility in CNS infiltrating pathogenic T_H17 cells, which indicate that this microRNA cluster might have some regulatory role in intestinal homeostatic T_H17 cells. And the regulatory region of *miR-155, miR-146, miR-17-92 cluster* and *miR-183-96-182* cluster was with the same chromatin accessibility between pathogenic and homeostatic T_H17 cells (Fig. 2a-b), many of them were already shown to be critical for effector $CD4^+$ T cell and Treg cell function[32, 39, 40, 41, 42].

Our group previously demonstrated that miR-21 expression was highly

upregulated in the inflamed CNS tissue of autoimmune EAE mice[43], a mouse model of human MS. A deep-sequencing survey of the miRNome in mouse $CD4^+$ helper T cell subsets derived in vitro showed high level of miR-21 in pathogenic T_H17 cells[34], and miR-21 expression accounted for almost 20% of total microRNA counts in T_H17 cells (Supplementary 2a-b). To better understand the regulation of miR-21 expression in T_H17 cells, we activated naive $CD4^+$ T cells in the presence of anti-CD3 and anti-CD28 with or without IL-6, IL-23, IL-1β or TGF-β1. Among the cytokines tested, IL-6 appeared to be a critical factor for miR-21 upregulation (Fig. 2c). IL-1β and IL-23 could further promote IL-6-induced miR-21 expression. IL-6 promotes T_H17 cell differentiation by activating Stat3, which directly drives the transcription of T_H17 lineage-specific genes, including *Rorc*, *Il17* and *Il23r*. We further validated these results by using *Stat3* conditional knockout mice in $CD4^+$ T cells (Fig. 2d). These data suggest that IL-6-STAT3 signaling is essential for miR-21 upregulation in pathogenic T_H17 cells.

T cell expression of miR-21 is critical for the maintenance of pathogenic T_H17 cells in vivo

We further studied the role of miR-21 in T_H17 cells by *miR-21*$^{-/-}$ mice. And we found normal T cell development and homeostasis in *miR-21*$^{-/-}$ mice. Then, we tested whether miR-21 was essential for naïve $CD4^+$ T cell activation and T_H17 cell differentiation in vitro. When activated with anti-CD3 and anti-CD28, CFSE-labeled *miR-21*$^{-/-}$ $CD4^+$ T cells proliferated normally just as control $CD4^+$ T cells,

which indicated that miR-21 was not essential for initial activation-induced proliferation of $CD4^+$ T cells (Supplementary Fig. 3a). Loss of miR-21 did not impact T_H17 cell differentiation induced by TGF-β1 and IL-6 (Supplementary Fig. 3b). It was reported that T_H17 cells could be induced by a combination of three inflammatory cytokines that is IL-6, IL-1β and IL-23, without exogenous TGF-β1[8, 13]. Interestingly, under this pathogenic T_H17 polarization condition, *miR-21*$^{-/-}$ $CD4^+$ T cells were less efficiently differentiated into T_H17 cells (Supplementary Fig. 3b-d). These results indicate that miR-21 is not essential for T_H17 cell differentiation induced by TGF-β1 and IL-6, however, it is required for the differentiation of T_H17 cells under IL-6/IL-1β/IL-23 condition.

At steady state, intestinal lamina propria provides a unique environment for the differentiation of T_H17 cells. IL-10 producing intestinal lamina propria T_H17 cells mediate mucosal defense and barrier tissue integrity[4]. To investigate the role of miR-21 in T_H17 cells under a more physiological condition, we checked the presence of intestinal lamina propria T_H17 cells in control and CD4-cre *miR-21*$^{f/f}$ mice (Fig. 3a, Supplementary Fig. 3e). We found that control and CD4-cre *miR-21*$^{f/f}$ mice have equivalent percentage of ileum $RORc^+$ $FoxP3^-$ T_H17 cells and $RORc^+$ Tregs in vivo (Fig. 3a-b), which suggest that T cell expression of miR-21 is largely dispensable for the development of T_H17 cells under homeostatic condition.

To assess whether IL-17-producing cells with a pathogenic phenotype were efficiently generated in vivo, we immunized control and CD4-cre *miR-21*$^{f/f}$ mice

with KLH emulsified in CFA subcutaneously. We observed no significant difference at day 5-7 post immunization (Fig. 3c-f). However, we observed significantly less T_H17 cells in CD4-cre *miR-21*$^{f/f}$ mice by day 10 in the draining LN after subcutaneously immunization (Fig. 3b-d). These results suggest that miR-21 is not required for the development of T_H17 cells under steady-state condition, however, it is essential for the maintenance of pathogenic T_H17 cells in vivo in a $CD4^+$ T cell intrinsic manner.

T cell expression of miR-21 is essential for pathogenic T_H17 cell mediated autoimmune disease

To determine the role of miR-21 in a pathogenic T_H17 cell dominant disease model, we performed passive EAE to specifically address the role of miR-21 in mediating CNS inflammation induced by pre-activated $MOG_{35–55}$-specific pathogenic T_H17 cells (Supplementary Fig. 4a-c). When adoptively transferred into naive recipient mice, only control MOG-specific T_H17 cells efficiently induced EAE (Supplementary Fig. 4d), *miR-21*$^{-/-}$ T_H17 cells failed to induce EAE, emphasizing an indispensable role of miR-21 in mediating the cell-intrinsic effector function of pathogenic T_H17 cells.

To exclude any possible role of miR-21 in dendritic cells and other myeloid cells that could contribute to EAE disease pathogenesis, we bred *miR-21*$^{f/+}$ allele to CD11c-cre and Lyz-cre, to delete miR-21 in dendritic cells, neutrophils, macrophages and microglia (Supplementary Fig. 4e-f). Loss of miR-21

expression in dendritic cell and myeloid cell compartment did not protect mice from autoantigen challenge (Fig. 4a). When immunized with MOG_{35-55} in CFA, CD4-cre *miR-21*$^{f/f}$ mice were highly resistant to EAE compared to littermate CD4-cre mice (Fig. 4b-e). At the peak of disease, CD4-cre *miR-21*$^{f/f}$ mice had less infiltrating of $CD4^+$ IL-17A$^+$ IFNγ$^+$ and IL17A$^+$ GM-CSF$^+$ pathogenic T_H17 cells. Taken together, these data clearly demonstrate that miR-21 mediates autoimmune disease through pathogenic T_H17 cells in a $CD4^+$ T cell intrinsic manner.

MiR-21 regulates metabolic adaptation of T_H17 cells under autoimmune inflammation

To better understand the general functional features of miR-21-deficient pathogenic T_H17 cells, we differentiated naïve T cells from control and *miR-21*$^{-/-}$ mice in vitro under pathogenic T_H17-skewing condition, RNA was extracted and subjected to RNA-seq to profile gene expression. We then analyzed the gene list for enrichment of gene ontology and canonical pathways using the DAVID bioinformatics databases[44]. In the absence of miR-21, T_H17 cells showed decreased expression of pathogenic T_H17 cell signature genes[11, 45], include lineage-specific transcription factors, cytokines, and cytokine receptors (Fig. 5a). Remarkably, many of the genes involved in glycolytic or related metabolic pathways were highly enriched, include key transporters for glucose intake, *Slc2a1/3*, and rate-limiting enzymes, *Hk1/2*, *Pfkl*, *Pgm2*, *Ldha* and *Pdk1* [18, 22] (Fig. 5a, Supplementary Fig. 5a). We further checked the glycolytic activity

of control and *miR-21*$^{-/-}$ pathogenic T_H17 cells by glycolysis stress test for extracellular acidification rate, both basal and maximal glycolytic capability were greatly decreased in *miR-21*$^{-/-}$ T_H17 cells compared to control T_H17 cells (Fig. 5b).

We further tested the metabolic potential of T_H17 (b) and T_H17 (23) cells, interestingly, we found pathogenic T_H17 (23) cells were much more glycolytic than non-pathogenic T_H17 (b) cells. T_H17 (23) cells express great more c-Myc, p-S6, HKII and Glut1 at the protein level, while express lower level of the metabolic repressor factor Foxo1 (Fig. 5c-d, Supplementary Fig. 5b). We further subjected T_H17 (b) and T_H17 (23) cells for high-resolution metabolomics analyses. Pathogenic T_H17 (23) cells were metabolically distinct from T_H17 (b) cells, and showed higher level of cytosol pyruvic acid, lactic acid, while T_H17 (b) cells showed higher level of citric acid (Fig. 5e, Supplementary Fig. 5c). Pathway analyses of altered metabolites by MetaboAnalyst showed that amino acid, amino sugar metabolism, and glycolytic intermediates trended higher in T_H17 (23) cells, but T_H17 (23) cells had lower amount of TCA metabolites and intermediates in purine metabolism (Fig. 5f).

Our data were consistent with the gene expression data from T_H17 cells derived in vivo, CNS infiltrating T_H17 cells were highly glycolytic compared to homeostatic LPL T_H17 cells[13, 14] (Supplementary Fig. 5d-e), of the upregulated ~3000 genes in CNS-derived T_H17 cells, 200 genes were implicated in metabolic pathways. Taken together, these data suggest that pathogenicity of

T_H17 cells were highly dependent on its metabolic activity, and miR-21 was a critical regulator of pathogenic T_H17 cell metabolic adaptation under autoimmune inflammation.

MiR-21 targets the E3 ligase Peli1-c-Rel pathway in pathogenic T_H17 cells

To further investigate the precise mechanism underlying how miR-21 promotes pathogenic T_H17 cell commitment and its metabolic function, we screened the direct targets of miR-21 by combining target prediction with Ago2 HITS-CLIP[46], TargetScan and RNA-seq data to identify overlapping gene transcripts (Supplementary Fig. 6a). Using a combination of these three approaches, we identified 5 common putative targets (*Esyt2*, *Mbnl1*, *Pdcd4*, *Peli1*, and *Psrc1*) (Fig. 6a). Among them, *Peli1* has been reported to function as a negative regulator of $CD4^+$ T cell activation by ubiquitination of c-Rel and *Peli1*$^{-/-}$ mice spontaneously developed autoimmune disease[47]. c-Rel was reported to be a metabolic regulator of germinal center B cell function[20, 21], and was critical for T_H17 cell differentiation[13, 48], therefore we chose *Peli1* for further analysis (Fig. 6a). By in vitro RNA immunoprecipitation assay, we found Ago2-immunoprecipitated RNAs had significantly reduced *Peli1* mRNA level in *miR-21*$^{-/-}$ T_H17 (23) cells (Fig. 6b-c), which suggests that *Peli1* is a functional target of miR-21 in pathogenic T_H17 cells. We further validated these at the protein level in purified GFP^+ T_H17 cells differentiated in vitro, we found that *miR-21*$^{-/-}$ T_H17 cells have significantly elevated level of Peli1 protein, whereas the protein level of c-Rel was significantly reduced in *miR-21*$^{-/-}$ T_H17 cells (Fig. 6d).

Interestingly, we found that T_H17 (23) cells expressed substantially high level of c-Rel compared to T_H17 (b) cells, and TGFβ1 signaling is required for the repression of c-Rel expression (Supplementary Fig. 6a-b). Taken together, these data suggest that miR-21 targets the Peli1-c-Rel pathway to promote the metabolic and effector function of pathogenic T_H17 cells.

Discussion

In the present study, we dissected the heterogeneity of T_H17 cells by genome wide epigenetic analysis. We found that T_H17 cells in vivo had discrete chromatin states. The regulatory region of key T_H17 cell-related transcription factors, metabolic regulators and microRNAs were with differential chromatin accessibility between homeostatic ileum T_H17 cells and CNS infiltrating T_H17 cells. Interestingly, colon T_H17 cells from *Citro Rodentium* infected mice had similar chromatin status with homeostatic ileum T_H17 cells, which indicates that they have similar anti-bacteria function in vivo.

In particular, we found the regulatory region of miR-21 was with great increased chromatin accessibility in CNS infiltrating T_H17 cells. We found that T_H17 cells expressed higher amount of miR-21, which was dependent on STAT3. We further show that IL-6, but not IL-23 or TGF-β1, serves a unique role to upregulate its expression, IL-1β and IL-23 together could further enhance its expression.

In the current study, we demonstrate that miR-21 was not essential for steady state intestinal LP T_H17 development; however, it was indispensable for the

maintenance of pathogenic T_H17 cell in vivo in a $CD4^+$ T cell intrinsic manner.

Higher miR-21 expression in the inflamed CNS tissue of autoimmune EAE mice has been observed in CNS infiltrating $CD4^+$ T cells, dendritic cells and other myeloid cells. In our study, we clearly demonstrated that miR-21 expression in $CD4^+$ T cells but not on dendritic cells were critically required for pathogenic T_H17 cell generation in vivo. CD4-cre *miR-21*$^{f/f}$ mice exhibited significantly lower disease incidence and severity. At the peak of disease, CD4-cre *miR-21*$^{f/f}$ mice had less infiltrating of $CD4^+$ IL-17A$^+$ IFNγ$^+$ and IL17A$^+$ GM-CSF$^+$ pathogenic T_H17 cells, whereas loss of miR-21 expression in dendritic cell and myeloid cell compartment did not protect mice from autoantigen challenge.

Although miR-21 was shown previously to be important in T_H17 cell generation[39], its exact action has not been well understood. In the current study, by using $CD4^+$ T cell conditional miR-21 knockout mice, we find that miR-21 is not required for the early stage T_H17 cell differentiation, but is critical for the maintenance of pathogenic T_H17 cells in vivo. We further demonstrate that miR-21$^{-/-}$ T_H17 cells express significantly less pathogenic T_H17 signature genes and key metabolism pathway genes. By globally metabolomics study we further demonstrated homeostatic T_H17 cells and pathogenic T_H17 cells had distinct metabolic status, with pathogenic T_H17 cells highly glycolytic. These data suggest that with increased chromatin openness of its regulatory region, miR-21 promotes metabolic adaptation of T_H17 cells under autoimmune inflammation.

To survey for putative targets of miR-21 in pathogenic T_H17 cells, we combined target prediction with previously reported miR-21 Ago HITS-CLIP data[46], TargetScan and our RNA-seq data to identify overlapping gene transcripts. Using a combination of these three approaches, we identified Peli1 as a functional target of miR-21 in pathogenic T_H17 cells. Peli1 has been reported to function as a negative regulator of $CD4^+$ T cell activation by ubiquitination of c-Rel and *Peli1*$^{-/-}$ mice spontaneously developed autoimmune disease.

To our knowledge, our study identifies the first evidence that by targeting key downstream regulators of TCR signaling miR-21 promotes the metabolic adaptation of T_H17 cells under autoimmune inflammation. Furthermore, the selective dependence of pathogenic T_H17 cells on miR-21–mediated metabolic reprogramming has provided novel targets for therapeutic intervention of autoimmune and pathogenic diseases elicited by T_H17 cells.

Methods

Mice

MiR-21$^{-/-}$ and *miR-21* $^{f/+}$ mice on the C57B6 background were from Biomodel Organism (Shanghai, China). CD4-cre, Lyz-cre, CD11c-cre and *Stat3* $^{f/+}$ mice were from Jackson lab. IL17A-eGFP reporter mice were from Biocytogen. All mice were maintained under specific pathogen-free conditions. All animal experiments were performed in compliance with the guide for the care and use of laboratory animals, and were approved by the institutional biomedical

research ethics committee of the Shanghai Institutes for Biological Sciences (Chinese Academy of Sciences).

Cell culture

Naïve $CD4^+$ T cells were isolated from lymph nodes or spleen of mice using a $CD4^+$ $CD62L^+$ T cell isolation kit II (Miltenyi Biotec) according to the manufacturer's instruction. Naïve $CD4^+$ T cells were stimulated with plate-bound anti-CD3ε mAb (5 μg/ml) in the presence of anti-CD28 mAb (2 μg/ml) in a 48-well plate under neutral conditions (10 μg/ml anti–IL-4 mAb and 10 μg/ml anti–IFN-γ mAb), IL-6 conditions (10 ng/ml IL-6, 10 μg/ml anti–IL-4 mAb, and 10 μg/ml anti–IFN-γ mAb), T_H17 (b) conditions (2 ng/ml TGF-β, 20 ng/ml IL-6, 10 μg/ml anti–IL-4 mAb, and 10 μg/ml anti–IFN-γ mAb), T_H17 (23) conditions (20 ng/ml IL-6, 20 ng/ml IL-1β, 20 ng/ml IL-23, 10 μg/ml anti–IL-4 mAb, and 10 μg/ml anti–IFN-γ mAb).

Antibodies and reagents

Antibodies to mouse CD3ε (145-2C11), CD28 (37.51), IL-4 (11B11), IFN-γ (XMG1.2), CD3ε PerCP5.5 (145-2C11), Foxp3 APC (FJK-16s), ROR gamma (t) PE (B2D) and GM-CSF PE (MP1-22E9) were from eBiosciences. Antibodies to mouse CD45 APC-cy7 (30-F11), CD4 BV510 (RM4-5), IL-17A PE (TC11-18H10), IFN-γ APC (XMG1.2) were from BD Biosciences. Recombinant Mouse IL-6, IL-1β, IL-23, and TGF-β1 protein were purchased from R&D Systems. Peli1 (F-7) was from Santa cruz, c-Rel (D4Y6M), Foxo1 (C29H4), p-S6 (2F9),

c-Myc (D3N8F), HKII (C64G5) were from Cell signaling. Glut1 (EPR3915) antibody was from Abcam. RIPAb+ Ago2 was from Merk millipore. XF Glycolysis Stress Test Kit was from Agilent technologies.

Intracellular cytokine staining

Cultured or tissue isolated lymphocytes were washed and stimulated with PMA (50 ng/ml) plus ionomycin (750 ng/ml) for 4 h at 37°C. Cells were stained with anti-CD45 APC-cy7, anti-CD3ε PerCP5.5 and anti-CD4 BV510 for 30 min at 4°C. Cells were then fixed, permeabilized with Perm/Wash buffer (BD), and stained with anti–IFN-γ APC, anti-GM-CSF PE or anti–IL-17A PE for 30 min at 4°C. Cytokine profiles of $CD4^{+}$ cells were analyzed on a FACSCalibur with FlowJo software (Tree Star).

Induction of EAE

IL17A-eGFP reporter mice, $CD4^{cre}$ miR-$21^{fl/fl}$ mice and littermate CD4-cre or miR-$21^{fl/fl}$ mice were injected subcutaneously in the tail base with MOG35-55 peptide (200 μg/mouse, MEVGWYRSPFSRVVHLYRNGK) in complete Freund's adjuvant. 5 min and 48 h after the injection of MOG35-55 peptide, the mice were injected intraperitoneally with pertussis toxin (200 ng/mouse; Sigma-Aldrich). Status of the mice was monitored and disease severity was scored three times a week as follows: 0 = no clinical signs, 1 = limp tail (tail paralysis), 2 = complete loss of tail tonicity or abnormal gait, 3 = partial hind limb paralysis, 4 = complete hind limb paralysis, 5 = forelimb paralysis or moribund, 6 = death.

Cells were isolated from whole brain and spinal cord at the peak of disease by Percoll gradient centrifugation (37%/70%) and subjected to flow cytometric analysis or flow cytometric sorting.

Citro Rodentium **infection**

C. rodentium strain DBS100 (ATCC51459; American Type Culture Collection) were prepared by shaking of bacteria overnight at 37 °C in Luria-Bertani broth. Bacterial cultures were serially diluted and plated on MacConkey agar plates so the CFU dose administered could be confirmed. For infection, IL17A-eGFP reporter mice were oral inoculated with 2×10^9 CFU C. rodentium in a total volume of 100 ul per mouse. T_H17 cells were isolated from colon tissue by Percoll gradient centrifugation (40%/80%) and subjected to flow cytometric sorting at day 7.

RNA-seq

Naive $CD4^+$ T cells from control and *miR-21*$^{-/-}$ mice were differentiated under pathogenic T_H17 (23) differentiation condition. Total RNA was prepared from these cells using Trizol reagent (Invitrogen). RNA-seq libraries were prepared using a SureSelect Strand Specific RNA Library Preparation kit (Agilent). Sequencing was performed on an Illumina HiSeq1500 using a TruSeq Rapid SBS kit (Illumina) in a 50-base single-end mode. mRNA profiles were calculated with a Cufflinks software and expressed as FPKM (fragments per kilobase of exon model per million mapped fragments).

ATAC-seq

ATAC-seq library preparations were performed as described[35]. In brief, 50,000 cells were washed in cold PBS and lysed. Transposition was performed at 37 °C for 30 min. After purification of the DNA with the MinElute PCR purification kit (Qiagen), DNA was amplified for 5 cycles. Additional PCR cycles were evaluated by real time PCR. Final product was cleaned by Ampure Beads at a 1.5× ratio. Libraries were sequenced on a Hiseq 2500 1T in a 50 bp/50 bp Paired end run, using the TruSeq SBS Kit v3 (Illumina).

Metabolomics

Metabolomic analyses were performed on an Agilent 7890A gas chromatography system coupled to an Agilent 5975C inert MSD system (Agilent Technologies)[49, 50]. MetaboAnalyst was used to analyze range-scale data and provide PCA and KEGG pathway analysis of metabolites significantly changed (www.metaboanalyst.ca/).

Statistics

Prism software was used for statistical analysis. Differences between groups were compared with an unpaired two-tailed t-test. A P value of less than 0.05 was considered statistically significant.

References

1. Littman DR, Rudensky AY. Th17 and regulatory T cells in mediating and restraining inflammation. *Cell* 2010, **140**(6)**:** 845-858.

2. Stockinger B, Omenetti S. The dichotomous nature of T helper 17 cells. *Nature reviews Immunology* 2017.

3. Ivanov, II, Atarashi K, Manel N, Brodie EL, Shima T, Karaoz U*, et al.* Induction of intestinal Th17 cells by segmented filamentous bacteria. *Cell* 2009, **139**(3)**:** 485-498.

4. Sano T, Huang W, Hall JA, Yang Y, Chen A, Gavzy SJ*, et al.* An IL-23R/IL-22 Circuit Regulates Epithelial Serum Amyloid A to Promote Local Effector Th17 Responses. *Cell* 2015, **163**(2)**:** 381-393.

5. Atarashi K, Tanoue T, Ando M, Kamada N, Nagano Y, Narushima S*, et al.* Th17 Cell Induction by Adhesion of Microbes to Intestinal Epithelial Cells. *Cell* 2015, **163**(2)**:** 367-380.

6. Zielinski CE, Mele F, Aschenbrenner D, Jarrossay D, Ronchi F, Gattorno M*, et al.* Pathogen-induced human TH17 cells produce IFN-gamma or IL-10 and are regulated by IL-1beta. *Nature* 2012, **484**(7395)**:** 514-518.

7. McGeachy MJ, Bak-Jensen KS, Chen Y, Tato CM, Blumenschein W, McClanahan T*, et al.* TGF-beta and IL-6 drive the production of IL-17 and IL-10 by T cells and restrain T(H)-17 cell-mediated pathology. *Nature immunology* 2007, **8**(12)**:** 1390-1397.

8. Ghoreschi K, Laurence A, Yang XP, Tato CM, McGeachy MJ, Konkel JE*, et al.* Generation of pathogenic T(H)17 cells in the absence of TGF-beta signalling. *Nature* 2010, **467**(7318)**:** 967-971.

9. El-Behi M, Ciric B, Dai H, Yan Y, Cullimore M, Safavi F*, et al.* The encephalitogenicity of T(H)17 cells is dependent on IL-1- and IL-23-induced production of the cytokine GM-CSF. *Nature immunology* 2011, **12**(6)**:** 568-575.

10. Codarri L, Gyulveszi G, Tosevski V, Hesske L, Fontana A, Magnenat L*, et al.* RORgammat drives production of the cytokine GM-CSF in helper T cells, which is essential for the effector phase of autoimmune neuroinflammation. *Nature immunology* 2011, **12**(6)**:** 560-567.

11. Wu C, Yosef N, Thalhamer T, Zhu C, Xiao S, Kishi Y*, et al.* Induction of pathogenic TH17

cells by inducible salt-sensing kinase SGK1. *Nature* 2013, **496**(7446)**:** 513-517.

12. Kleinewietfeld M, Manzel A, Titze J, Kvakan H, Yosef N, Linker RA*, et al.* Sodium chloride drives autoimmune disease by the induction of pathogenic TH17 cells. *Nature* 2013, **496**(7446)**:** 518-522.

13. Gaublomme JT, Yosef N, Lee Y, Gertner RS, Yang LV, Wu C*, et al.* Single-Cell Genomics Unveils Critical Regulators of Th17 Cell Pathogenicity. *Cell* 2015, **163**(6)**:** 1400-1412.

14. Wang C, Yosef N, Gaublomme J, Wu C, Lee Y, Clish CB*, et al.* CD5L/AIM Regulates Lipid Biosynthesis and Restrains Th17 Cell Pathogenicity. *Cell* 2015, **163**(6)**:** 1413-1427.

15. Buck MD, O'Sullivan D, Pearce EL. T cell metabolism drives immunity. *The Journal of experimental medicine* 2015, **212**(9)**:** 1345-1360.

16. Man K, Kallies A. Synchronizing transcriptional control of T cell metabolism and function. *Nature reviews Immunology* 2015, **15**(9)**:** 574-584.

17. Pollizzi KN, Powell JD. Integrating canonical and metabolic signalling programmes in the regulation of T cell responses. *Nature reviews Immunology* 2014, **14**(7)**:** 435-446.

18. Wang R, Dillon CP, Shi LZ, Milasta S, Carter R, Finkelstein D*, et al.* The transcription factor Myc controls metabolic reprogramming upon T lymphocyte activation. *Immunity* 2011, **35**(6)**:** 871-882.

19. Verbist KC, Guy CS, Milasta S, Liedmann S, Kaminski MM, Wang R*, et al.* Metabolic maintenance of cell asymmetry following division in activated T lymphocytes. *Nature* 2016, **532**(7599)**:** 389-393.

20. Boothby M, Rickert RC. Metabolic Regulation of the Immune Humoral Response. *Immunity* 2017, **46**(5)**:** 743-755.

21. Heise N, De Silva NS, Silva K, Carette A, Simonetti G, Pasparakis M*, et al.* Germinal center B cell maintenance and differentiation are controlled by distinct NF-kappaB transcription factor subunits. *The Journal of experimental medicine* 2014, **211**(10)**:** 2103-2118.

22. Shi LZ, Wang R, Huang G, Vogel P, Neale G, Green DR*, et al.* HIF1alpha-dependent glycolytic pathway orchestrates a metabolic checkpoint for the differentiation of TH17 and Treg cells. *The Journal of experimental medicine* 2011, **208**(7)**:** 1367-1376.

23. Wilhelm K, Happel K, Eelen G, Schoors S, Oellerich MF, Lim R*, et al.* FOXO1 couples metabolic activity and growth state in the vascular endothelium. *Nature* 2016, **529**(7585)**:** 216-220.

24. Angelin A, Gil-de-Gomez L, Dahiya S, Jiao J, Guo L, Levine MH, *et al.* Foxp3 Reprograms T Cell Metabolism to Function in Low-Glucose, High-Lactate Environments. *Cell metabolism* 2017.

25. Ho PC, Bihuniak JD, Macintyre AN, Staron M, Liu X, Amezquita R, *et al.* Phosphoenolpyruvate Is a Metabolic Checkpoint of Anti-tumor T Cell Responses. *Cell* 2015, **162**(6)**:** 1217-1228.

26. Chang CH, Qiu J, O'Sullivan D, Buck MD, Noguchi T, Curtis JD, *et al.* Metabolic Competition in the Tumor Microenvironment Is a Driver of Cancer Progression. *Cell* 2015, **162**(6)**:** 1229-1241.

27. Mehta A, Baltimore D. MicroRNAs as regulatory elements in immune system logic. *Nature reviews Immunology* 2016, **16**(5)**:** 279-294.

28. Boldin MP, Taganov KD, Rao DS, Yang L, Zhao JL, Kalwani M, *et al.* miR-146a is a significant brake on autoimmunity, myeloproliferation, and cancer in mice. *The Journal of experimental medicine* 2011, **208**(6)**:** 1189-1201.

29. Rodriguez A, Vigorito E, Clare S, Warren MV, Couttet P, Soond DR, *et al.* Requirement of bic/microRNA-155 for normal immune function. *Science (New York, NY)* 2007, **316**(5824)**:** 608-611.

30. Thai TH, Calado DP, Casola S, Ansel KM, Xiao C, Xue Y, *et al.* Regulation of the germinal center response by microRNA-155. *Science (New York, NY)* 2007, **316**(5824)**:** 604-608.

31. O'Connell RM, Kahn D, Gibson WS, Round JL, Scholz RL, Chaudhuri AA, *et al.* MicroRNA-155 promotes autoimmune inflammation by enhancing inflammatory T cell development. *Immunity* 2010, **33**(4)**:** 607-619.

32. Escobar TM, Kanellopoulou C, Kugler DG, Kilaru G, Nguyen CK, Nagarajan V, *et al.* miR-155 activates cytokine gene expression in Th17 cells by regulating the DNA-binding protein Jarid2 to relieve polycomb-mediated repression. *Immunity* 2014, **40**(6)**:** 865-879.

33. Hu R, Kagele DA, Huffaker TB, Runtsch MC, Alexander M, Liu J, *et al.* miR-155 promotes T follicular helper cell accumulation during chronic, low-grade inflammation. *Immunity* 2014, **41**(4)**:** 605-619.

34. Ichiyama K, Gonzalez-Martin A, Kim BS, Jin HY, Jin W, Xu W, *et al.* The MicroRNA-183-96-182 Cluster Promotes T Helper 17 Cell Pathogenicity by Negatively Regulating Transcription Factor Foxo1 Expression. *Immunity* 2016, **44**(6)**:** 1284-1298.

35. Buenrostro JD, Giresi PG, Zaba LC, Chang HY, Greenleaf WJ. Transposition of native

chromatin for fast and sensitive epigenomic profiling of open chromatin, DNA-binding proteins and nucleosome position. *Nature methods* 2013, **10**(12)**:** 1213-1218.

36. van der Veeken J, Gonzalez AJ, Cho H, Arvey A, Hemmers S, Leslie CS*, et al.* Memory of Inflammation in Regulatory T Cells. *Cell* 2016, **166**(4)**:** 977-990.

37. Ceribelli M, Hou ZE, Kelly PN, Huang DW, Wright G, Ganapathi K*, et al.* A Druggable TCF4- and BRD4-Dependent Transcriptional Network Sustains Malignancy in Blastic Plasmacytoid Dendritic Cell Neoplasm. *Cancer cell* 2016, **30**(5)**:** 764-778.

38. Philip M, Fairchild L, Sun L, Horste EL, Camara S, Shakiba M*, et al.* Chromatin states define tumour-specific T cell dysfunction and reprogramming. *Nature* 2017, **545**(7655)**:** 452-456.

39. Murugaiyan G, da Cunha AP, Ajay AK, Joller N, Garo LP, Kumaradevan S*, et al.* MicroRNA-21 promotes Th17 differentiation and mediates experimental autoimmune encephalomyelitis. *The Journal of clinical investigation* 2015, **125**(3)**:** 1069-1080.

40. Pua HH, Steiner DF, Patel S, Gonzalez JR, Ortiz-Carpena JF, Kageyama R*, et al.* MicroRNAs 24 and 27 Suppress Allergic Inflammation and Target a Network of Regulators of T Helper 2 Cell-Associated Cytokine Production. *Immunity* 2016, **44**(4)**:** 821-832.

41. Pan W, Zhu S, Dai D, Liu Z, Li D, Li B*, et al.* MiR-125a targets effector programs to stabilize Treg-mediated immune homeostasis. *Nature communications* 2015, **6:** 7096.

42. Cho S, Wu CJ, Yasuda T, Cruz LO, Khan AA, Lin LL*, et al.* miR-23 approximately 27 approximately 24 clusters control effector T cell differentiation and function. *The Journal of experimental medicine* 2016, **213**(2)**:** 235-249.

43. Zhu S, Pan W, Song X, Liu Y, Shao X, Tang Y*, et al.* The microRNA miR-23b suppresses IL-17-associated autoimmune inflammation by targeting TAB2, TAB3 and IKK-alpha. *Nature medicine* 2012, **18**(7)**:** 1077-1086.

44. Huang da W, Sherman BT, Lempicki RA. Systematic and integrative analysis of large gene lists using DAVID bioinformatics resources. *Nature protocols* 2009, **4**(1)**:** 44-57.

45. Ciofani M, Madar A, Galan C, Sellars M, Mace K, Pauli F*, et al.* A validated regulatory network for Th17 cell specification. *Cell* 2012, **151**(2)**:** 289-303.

46. Loeb GB, Khan AA, Canner D, Hiatt JB, Shendure J, Darnell RB*, et al.* Transcriptome-wide miR-155 binding map reveals widespread noncanonical microRNA targeting. *Molecular cell* 2012, **48**(5)**:** 760-770.

47. Chang M, Jin W, Chang JH, Xiao Y, Brittain GC, Yu J*, et al.* The ubiquitin ligase Peli1 negatively regulates T cell activation and prevents autoimmunity. *Nature immunology* 2011, **12**(10)**:** 1002-1009.

48. Ruan Q, Kameswaran V, Zhang Y, Zheng S, Sun J, Wang J*, et al.* The Th17 immune response is controlled by the Rel-RORgamma-RORgamma T transcriptional axis. *The Journal of experimental medicine* 2011, **208**(11)**:** 2321-2333.

49. Sellick CA, Hansen R, Stephens GM, Goodacre R, Dickson AJ. Metabolite extraction from suspension-cultured mammalian cells for global metabolite profiling. *Nature protocols* 2011, **6**(8)**:** 1241-1249.

50. Jin H, Qiao F, Chen L, Lu C, Xu L, Gao X. Serum metabolomic signatures of lymph node metastasis of esophageal squamous cell carcinoma. *Journal of proteome research* 2014, **13**(9)**:** 4091-4103.

Acknowledgments

We thank Youcun Qian for kindly sharing with us *C. rodentium* strain DBS100.

Contributions

X.Y. and N.S. designed the experiments and wrote the manuscript; X.Y. did most of the experiments; L.W. helped with the mouse experiments; C.Y. and R. Q. helped with the ATAC-seq data analysis; Y.C. helped with cell culture.

Competing interests

The authors declare no competing financial interests.

Fig. Legends

Fig.1 T_H17 Cells show great discrete chromatin states in vivo

(a) Scatterplots of mean ATAC-seq counts per peak comparing the indicated samples.

(b) Scatterplots of mean ATAC-seq counts per peak comparing the indicated samples.

(c) Principal component analysis (PCA) of peak accessibility in ileum (blue), colon *Citrobacter* (yellow) and CNS (red) T_H17 cells.

(d) ATAC-seq signal profiles across *Batf*, *Irf4*, *Ahr* and *c-Maf* loci.

Fig. 2 IL-6 and STAT3-dependent activation of miR-21 in pathogenic T_H17 cells

(a) ATAC-seq signal profiles across *miR-155hg*, *miR-146*, *miR-17-92* cluster and *miR-183-96-182* cluster loci.

(b) ATAC-seq signal profiles across *miR-21*, *miR-23a* cluster, *miR-210* and *miR-125a* cluster loci.

(c) Relative expression of miR-21 by in vitro cytokine stimulation.

(a) Relative expression of miR-21 in $CD4^+$ T cells from CD4-cre and CD4-cre *Stat3*$^{f/f}$ mice, activated with anti-CD3/anti-CD28 and stimulated with IL-6, IL-1b and IL-23. *P < 0.05 (unpaired t-test). Data are from one experiment representative of two independent experiments (mean and s. d. in c, d).

Fig. 3 T cell expression of miR-21 is critical for the maintenance of pathogenic T_H17 cells in vivo

(a) Flow cytometry of $CD4^+$ T cells from 7-week old naïve CD4-cre and CD4-cre *miR-21*$^{f/f}$ mice (n=3) ileum lamina propria, numbers in quadrants indicate percent cells in each.

(b) Percentage of $RORc^+$ $FOXP3^-$ T_H17 cells, $RORc^+$ $FOXP3^+$ and $RORc^-$ $FOXP3^+$ Treg cells from ileum lamia propria of CD4-cre and CD4-cre *miR-21*$^{f/f}$ mice as in (a).

(c) Flow cytometry of draining lymph nodes $CD4^+$ T cells from CD4-cre and CD4-cre *miR-21*$^{f/f}$ mice (n=4) on day 7 after immunized with KLH in CFA and restimulated with KLH for overnight, numbers adjacent to outlined areas indicate percent $CD44^+$ IL-$17A^+$ cells.

(d) Flow cytometry of draining lymph nodes $CD4^+$ T cells from CD4-cre and CD4-cre *miR-21*$^{f/f}$ mice (n=4) on day 10 after immunized with KLH in CFA and restimulated with KLH for overnight, numbers adjacent to outlined areas indicate percent $CD44^+$ IL-$17A^+$ cells.

(e) Percentage of $CD44^+$ IL-$17A^+$ cells as in (d).

(f) Numbers of $CD44^+$ IL-$17A^+$ cells as in (d). *$P < 0.05$ (unpaired t-test). Data are from one experiment representative of two independent experiments (mean and s. d. in c, d).

Fig. 4 T cell expression of miR-21 is essential for T_H17 cell-mediated autoimmune disease

(a) EAE development in CD4-cre and CD4-cre *miR-21*$^{f/f}$ (n=5) mice.

(b) EAE development in Lyz2-cre and Lyz2-cre *miR-21*$^{f/f}$ (n=7) mice.

(c) EAE development in CD11c-cre and CD11c-cre *miR-21*$^{f/f}$ (n=7) mice.

(d) Flow cytometry of IL-17A and IFN-γ secretion by CD4^{+} T cells isolated from spinal cord of CD4-cre and CD4-cre *miR-21*$^{f/f}$ mice at the peak of disease (n = 4).

(e) Flow cytometry of IL-17A and GM-CSF secretion by CD4^{+} T cells isolated from spinal cord of CD4-cre and CD4-cre *miR-21*$^{f/f}$ mice at the peak of disease (n = 4).

(f) Percentage of IL17A^{+} IFN-γ^{-}, IL17A^{+} IFN-γ^{+} and IL17A^{-} IFN-γ^{+} cells from spinal cord of CD4-cre and CD4-cre *miR-21*$^{f/f}$ mice as in (d).

(g) Percentage of IL17A^{+} GM-CSF^{-}, IL17A^{+} GM-CSF^{+} and IL17A^{-} GM-CSF^{+} cells from spinal cord of CD4-cre and CD4-cre *miR-21*$^{f/f}$ mice as in (e). *P < 0.05 (unpaired t-test). Data are from one experiment representative of three independent experiments (mean and s. d. in c, d).

Fig. 5 MiR-21 regulates metabolic adaptation of T_H17 cells under autoimmune inflammation

(a) Heat map of selected genes of interest in T_H17 cell pathogenicity (left) and in glycolytic pathways (right).

(b) Extracellular acidification rate (ECAR) of T_H17 (23) cells differentiated from control and *miR-21*$^{-/-}$ mice for 96 hs assessed by a glycolysis stress test.

(c) Western blot analysis of Foxo1, c-Myc and p-S6 in total protein from T_H17 (b) and T_H17 (23) cells differentiated in vitro for indicated time.

(d) Western blot analysis of HKII and Glut1 in total protein from T_H17 (b) and

T_H17 (23) cells differentiated in vitro for indicated time.

(e) Metabolomics analysis of T_H17 (b) and T_H17 (23) cells differentiated in vitro for 48 hs, the top differentially observed metabolites are shown in heat map.

(f) Pathway impact of metabolic pathways that most discriminate T_H17 (23) cells from T_H17 (b) cells. Data are from one experiment representative of two independent experiments (b), >3 independent experiments (c, d).

Fig. 6 MiR-21 targets the E3 ligase Peli1-c-Rel pathway in pathogenic T_H17 cells

a) Comparison of gene list from RNA-seq, Targetscan and CLIP-seq data, showing an overlap of 5 potential miR-21 target genes.

b) RT-PCR analysis of enriched Peli1 mRNA from Ago2 immunoprecipitated total RNA from in vitro differentiated Control and *miR-21*$^{-/-}$ T_H17(23) cells.

c) The 3' UTR of Peli1 in activated $CD4^+$ T cells from HITS-CLIP data[46].

d) Western blot analysis of Peli1 and c-Rel from sorted GFP^+ T_H17 cells differentiated under indicated condition.

Fig. 1

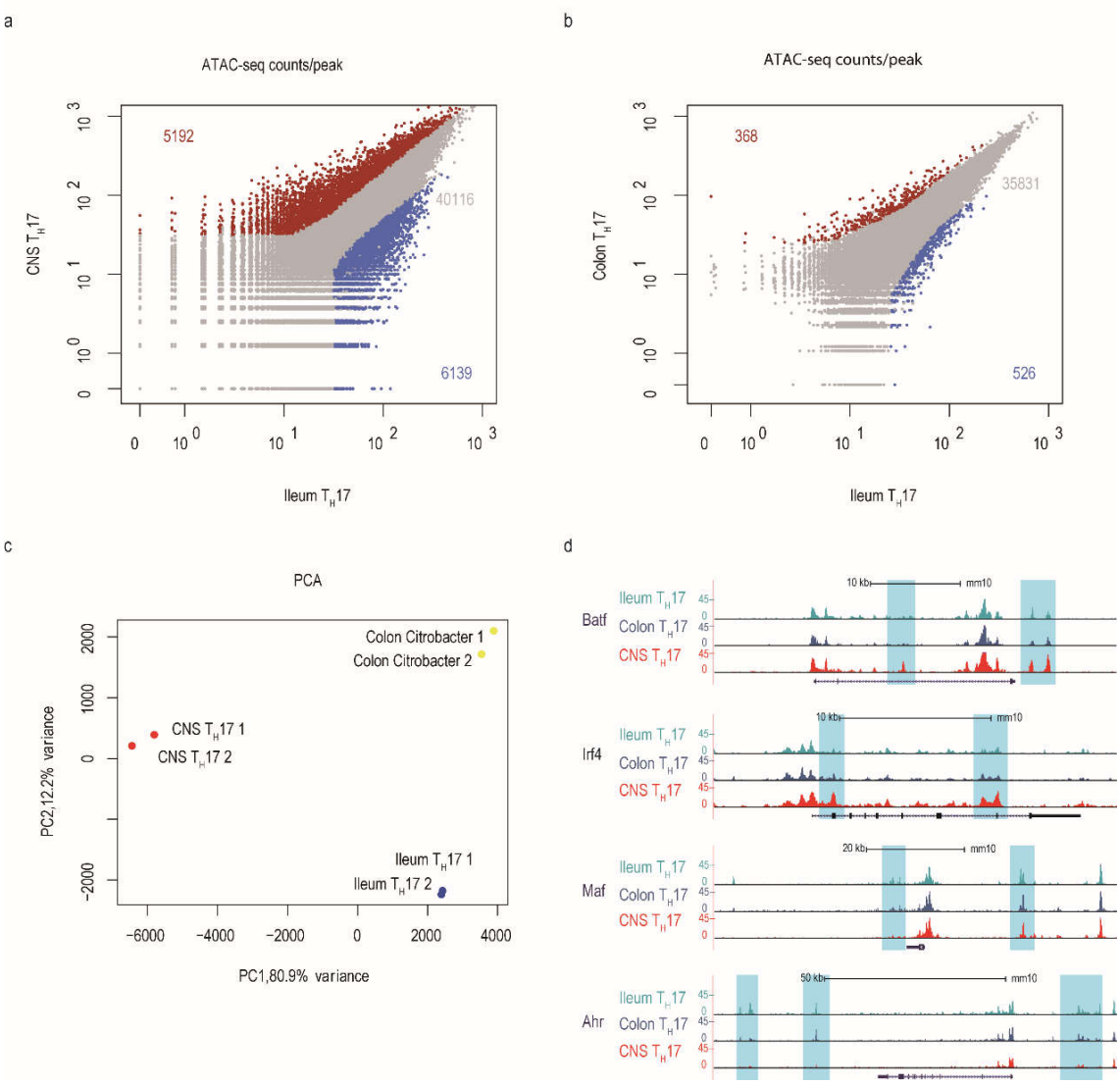
a
ATAC-seq counts/peak
5192
40116
6139
CNS T_H17
Ileum T_H17
b
ATAC-seq counts/peak
368
35831
526
Colon T_H17
Ileum T_H17
c
PCA
Colon Citrobacter 1
Colon Citrobacter 2
CNS T_H17 1
CNS T_H17 2
Ileum T_H17 1
Ileum T_H17 2
PC2,12.2% variance
PC1,80.9% variance
d
Batf
Irf4
Maf
Ahr
Ileum T_H17
Colon T_H17
CNS T_H17
10 kb
20 kb
50 kb
mm10

Fig. 2

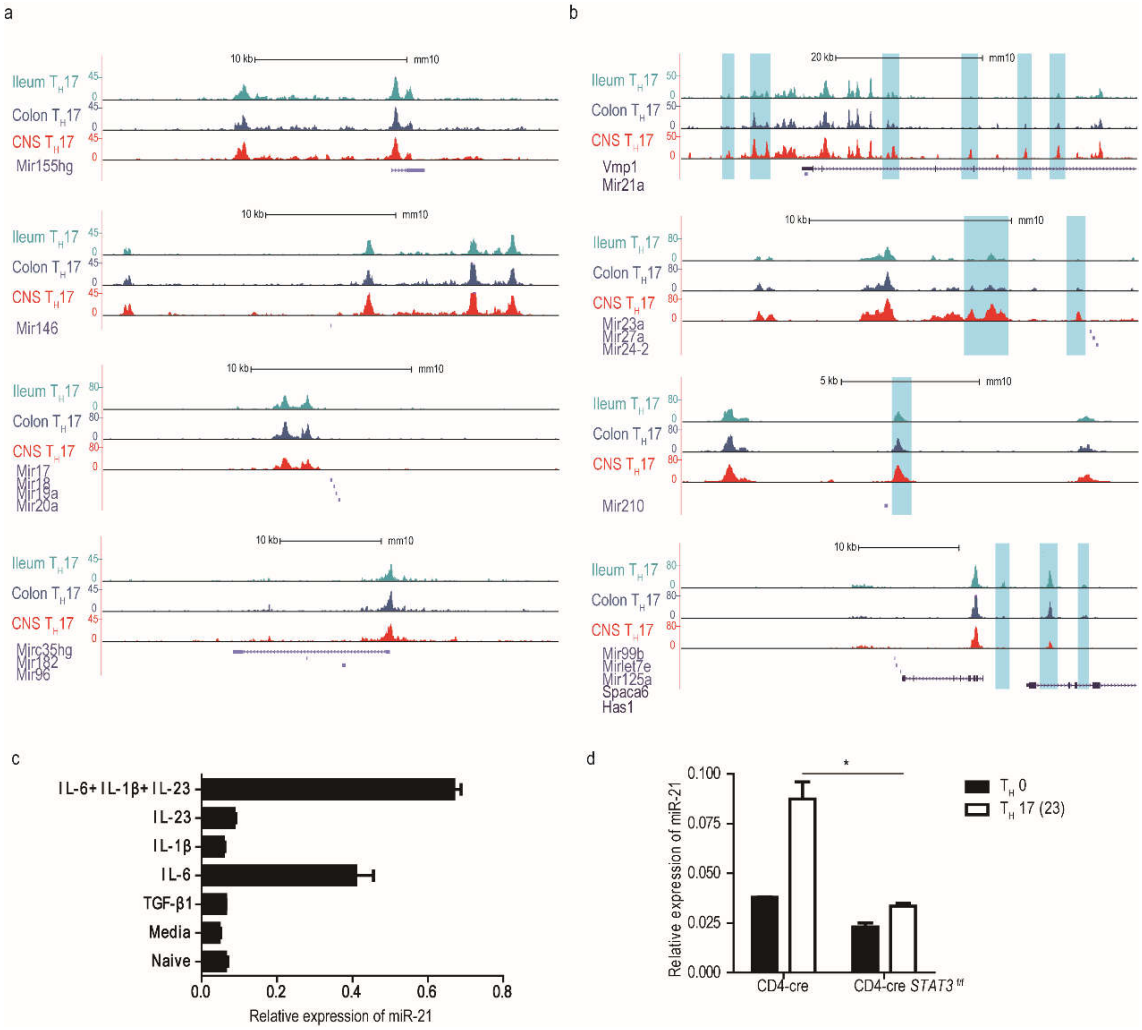
a
b
Ileum T_H17
Colon T_H17
CNS T_H17
Mir155hg
Mir146
Mir17
Mir18
Mir19a
Mir20a
Mirc35hg
Mir182
Mir96
Vmp1
Mir21a
Mir23a
Mir27a
Mir24-2
Mir210
Mir99b
Mirlet7e
Mir125a
Spaca6
Has1
10 kb
20 kb
5 kb
mm10
c
IL-6+IL-1β+IL-23
IL-23
IL-1β
IL-6
TGF-β1
Media
Naive
0.0
0.2
0.4
0.6
0.8
Relative expression of miR-21
d
Relative expression of miR-21
0.100
0.075
0.050
0.025
0.000
CD4-cre
CD4-cre STAT3 f/f
T_H0
T_H17 (23)
*

Fig. 3

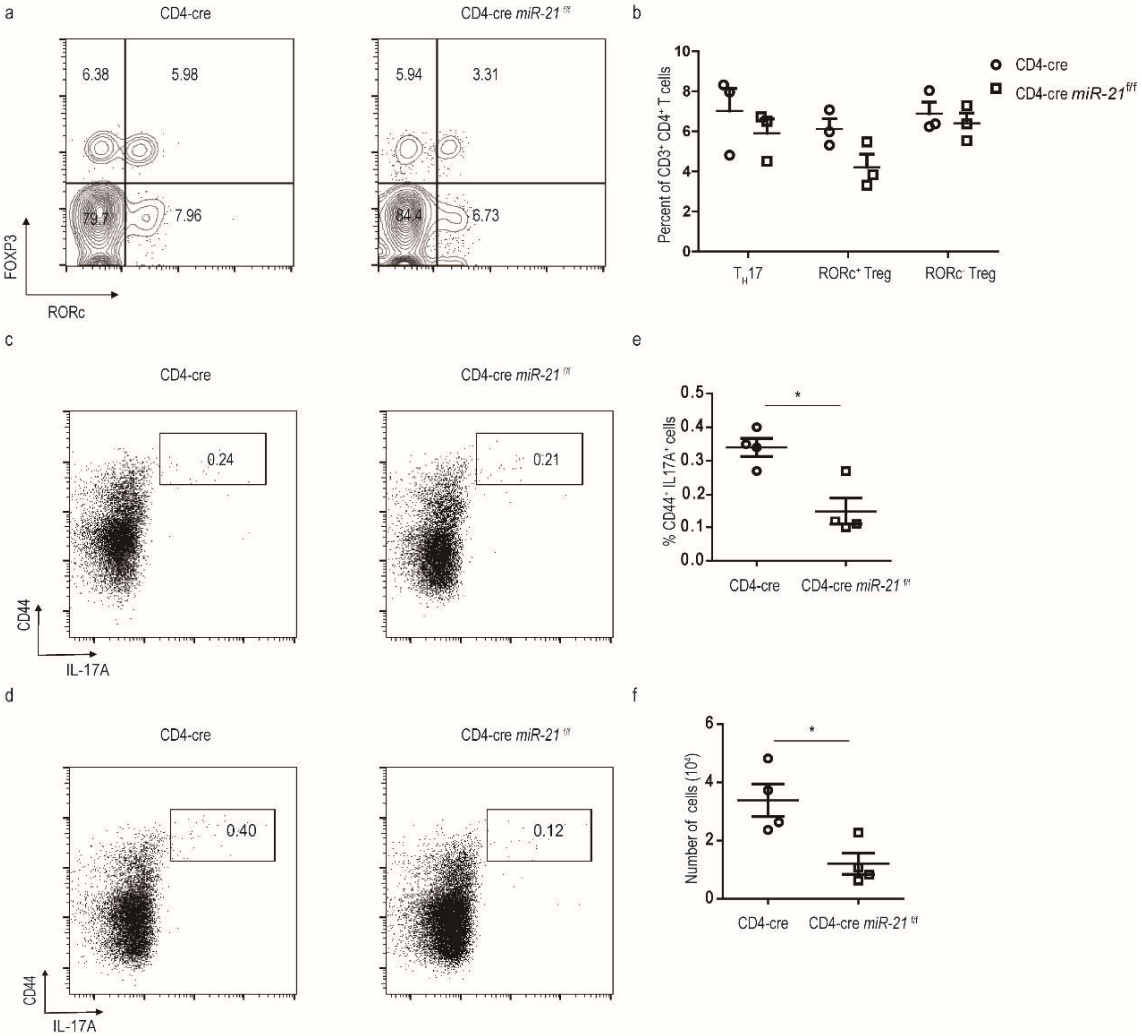
a
CD4-cre
CD4-cre miR-21 f/f
6.38
5.98
79.7
7.96
5.94
3.31
84.4
6.73
FOXP3
RORc
b
Percent of CD3+ CD4+ T cells
CD4-cre
CD4-cre miR-21f/f
TH17
RORc+ Treg
RORc- Treg
c
CD4-cre
CD4-cre miR-21 f/f
0.24
0.21
CD44
IL-17A
e
% CD44+ IL17A+ cells
*
CD4-cre
CD4-cre miR-21 f/f
d
CD4-cre
CD4-cre miR-21 f/f
0.40
0.12
CD44
IL-17A
f
Number of cells (10⁶)
*
CD4-cre
CD4-cre miR-21 f/f

Fig. 4

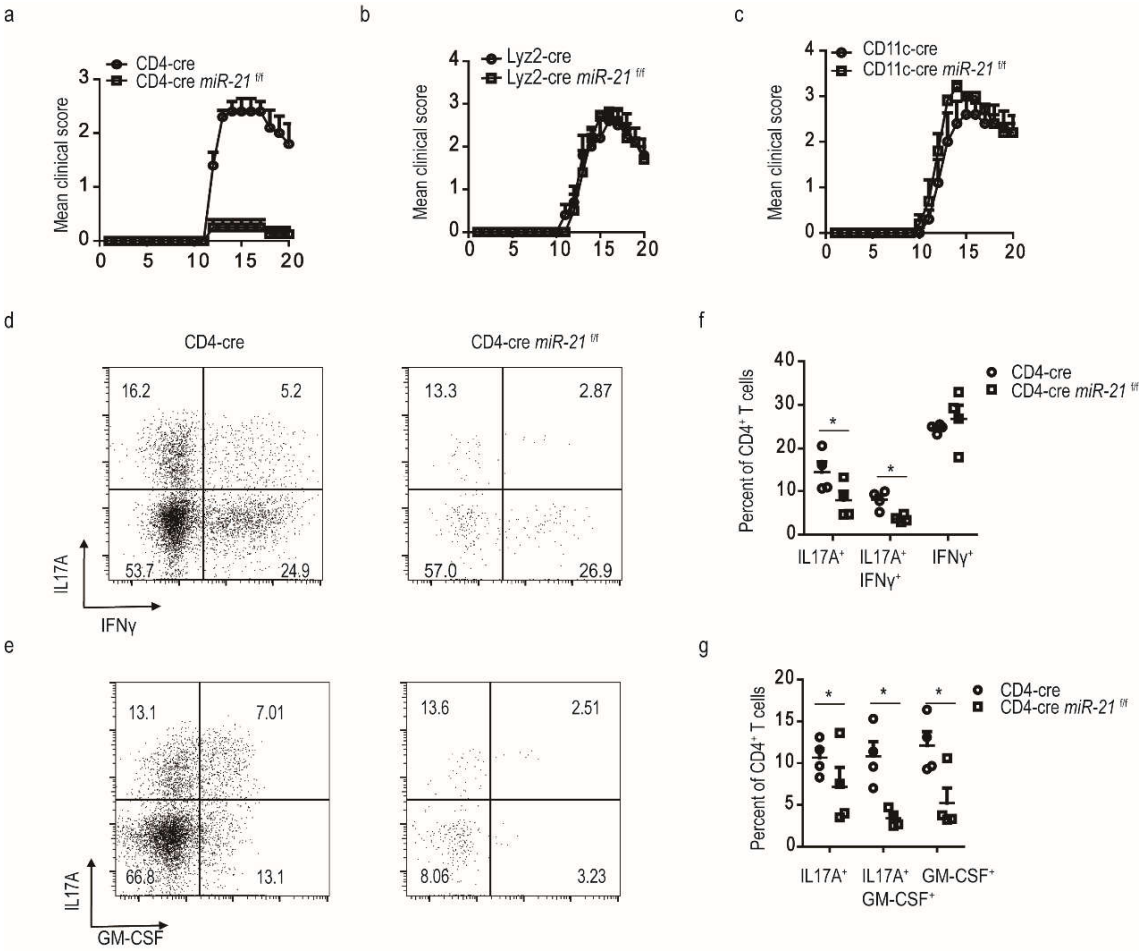
a
CD4-cre
CD4-cre miR-21 f/f
Mean clinical score
b
Lyz2-cre
Lyz2-cre miR-21 f/f
Mean clinical score
c
CD11c-cre
CD11c-cre miR-21 f/f
Mean clinical score
d
CD4-cre
CD4-cre miR-21 f/f
16.2
5.2
53.7
24.9
13.3
2.87
57.0
26.9
IL17A
IFNγ
e
13.1
7.01
66.8
13.1
13.6
2.51
8.06
3.23
IL17A
GM-CSF
f
Percent of CD4+ T cells
CD4-cre
CD4-cre miR-21 f/f
IL17A+
IL17A+ IFNγ+
IFNγ+
g
Percent of CD4+ T cells
CD4-cre
CD4-cre miR-21 f/f
IL17A+
IL17A+ GM-CSF+
GM-CSF+

Fig. 5

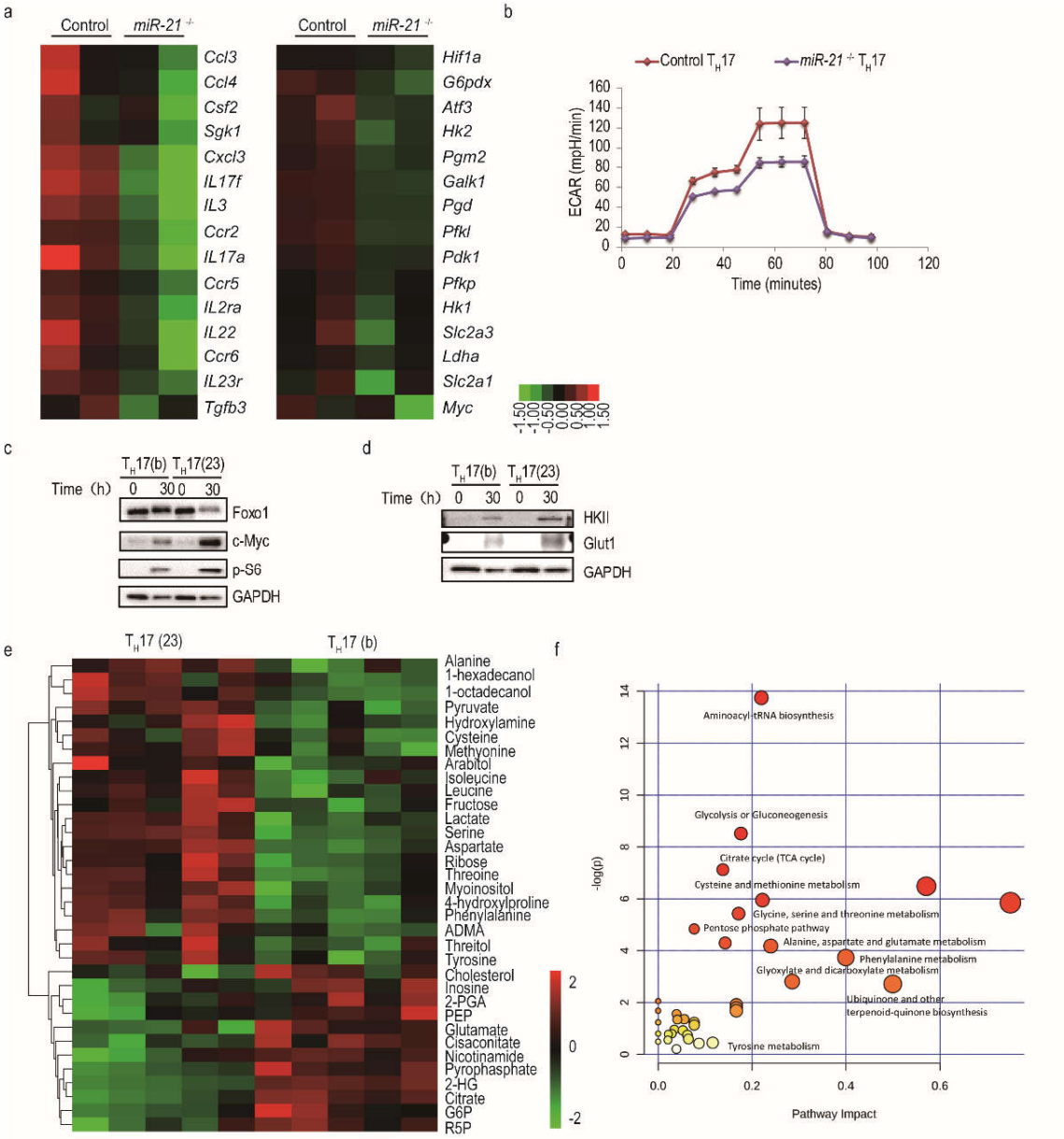
a
Control
miR-21 -/-
Ccl3
Ccl4
Csf2
Sgk1
Cxcl3
IL17f
IL3
Ccr2
IL17a
Ccr5
IL2ra
IL22
Ccr6
IL23r
Tgfb3
Hif1a
G6pdx
Atf3
Hk2
Pgm2
Galk1
Pgd
Pfkl
Pdk1
Pfkp
Hk1
Slc2a3
Ldha
Slc2a1
Myc
b
Control TH17
miR-21 -/- TH17
ECAR (mpH/min)
Time (minutes)
c
TH17(b) TH17(23)
Time (h) 0 30 0 30
Foxo1
c-Myc
p-S6
GAPDH
d
TH17(b) TH17(23)
Time (h) 0 30 0 30
HKII
Glut1
GAPDH
e
TH17 (23)
TH17 (b)
Alanine
1-hexadecanol
1-octadecanol
Pyruvate
Hydroxylamine
Cysteine
Methyonine
Arabitol
Isoleucine
Leucine
Fructose
Lactate
Serine
Aspartate
Ribose
Threoine
Myoinositol
4-hydroxylproline
Phenylalanine
ADMA
Threitol
Tyrosine
Cholesterol
Inosine
2-PGA
PEP
Glutamate
Cisaconitate
Nicotinamide
Pyrophasphate
2-HG
Citrate
G6P
R5P
f
Aminoacyl-tRNA biosynthesis
Glycolysis or Gluconeogenesis
Citrate cycle (TCA cycle)
Cysteine and methionine metabolism
Glycine, serine and threonine metabolism
Pentose phosphate pathway
Alanine, aspartate and glutamate metabolism
Phenylalanine metabolism
Glyoxylate and dicarboxylate metabolism
Ubiquinone and other terpenoid-quinone biosynthesis
Tyrosine metabolism
-log(p)
Pathway Impact

Fig. 6

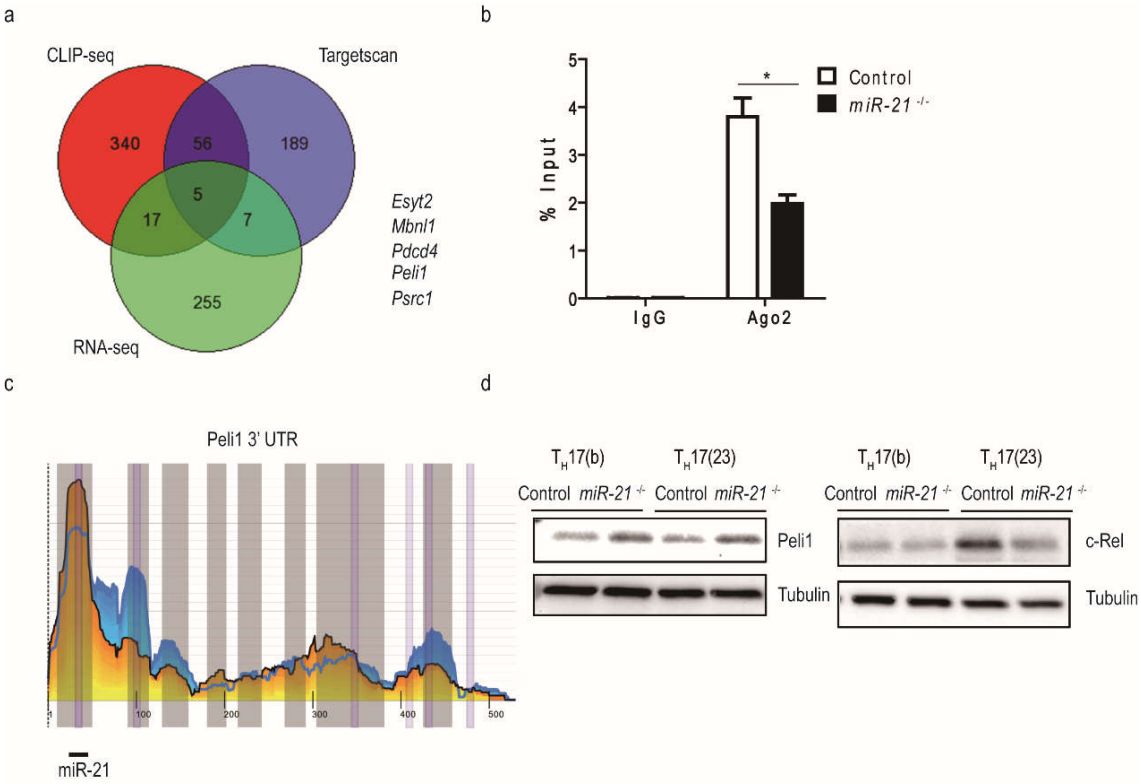
a
CLIP-seq
Targetscan
RNA-seq
340
56
189
5
17
7
255
Esyt2
Mbnl1
Pdcd4
Peli1
Psrc1
b
% Input
Control
miR-21 -/-
IgG
Ago2
c
Peli1 3' UTR
miR-21
d
TH17(b)
TH17(23)
Control
miR-21 -/-
Peli1
Tubulin
c-Rel

Supplementary Figures

Supplementary Fig. 1

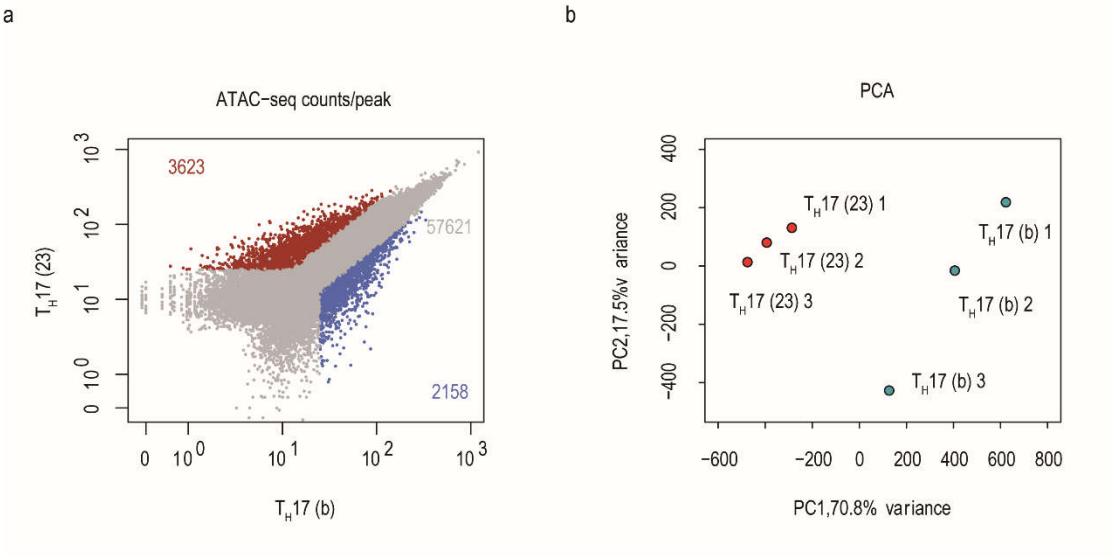

Supplementary Fig. 1 In vitro-derived T_H17 Cells show great discrete chromatin states

(e) Scatterplots of mean ATAC-seq counts per peak comparing the indicated samples.

(f) Principal component analysis (PCA) of peak accessibility in non-pathogenic T_H17(b) and pathogenic T_H17(23) cells.

Supplementary Fig. 2

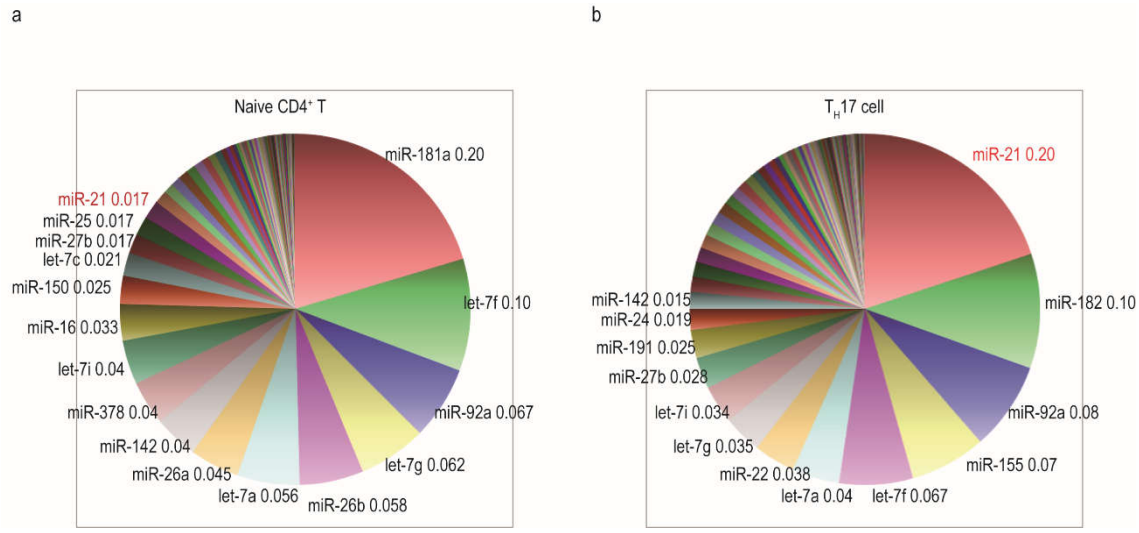

Supplementary Fig. 2 Expression of miR-21 in in vitro-derived T_H17 Cells

Pie charts demonstrate the percentage of reads of indicated microRNA in total microRNA reads of naïve $CD4^+$ T cell (a) and sorted T_H17 cells (b). The microRNA sequencing data was from ref[34].

Supplementary Fig. 3

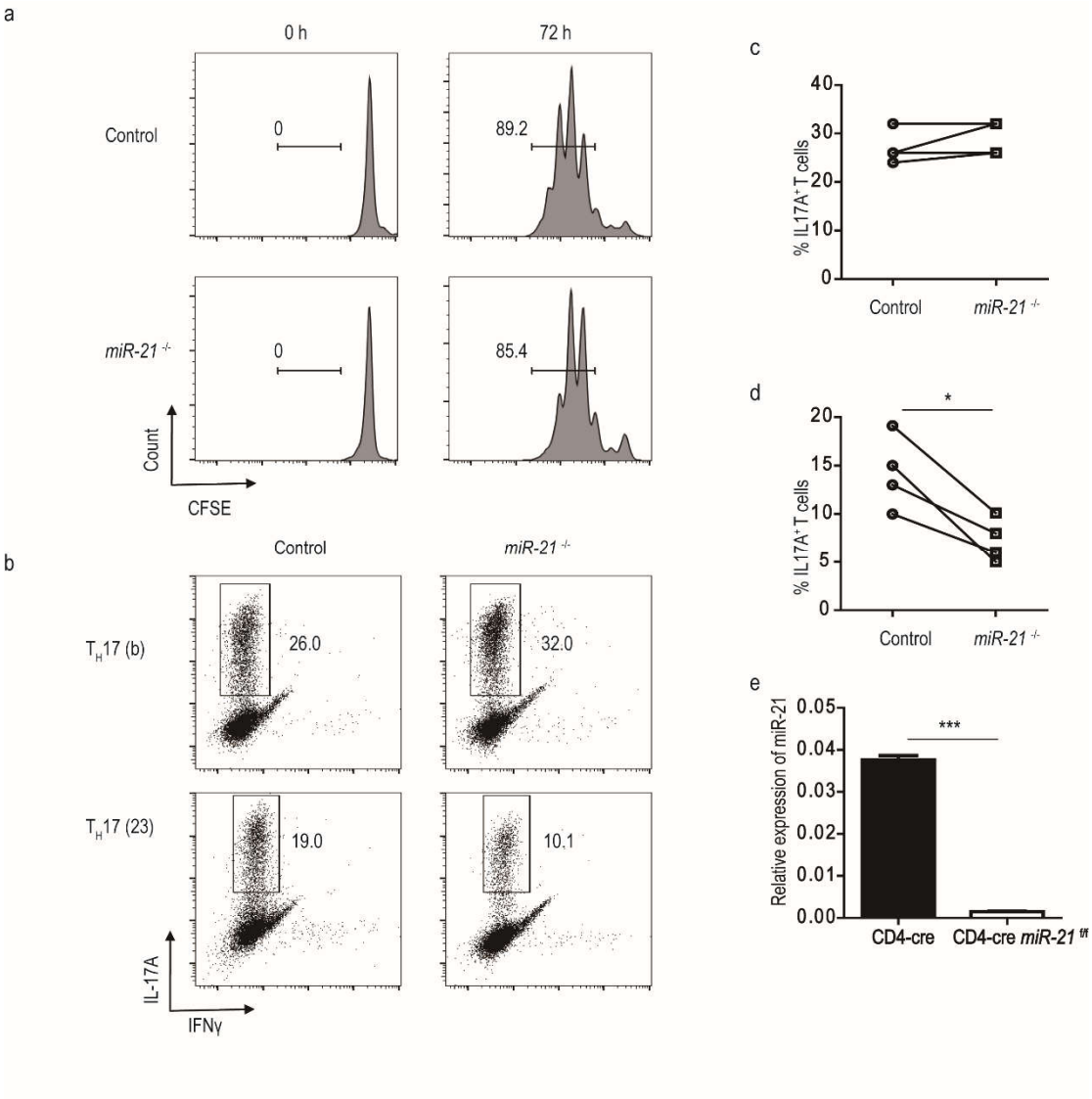

Supplementary Fig. 3 MiR-21 is essential for pathogenic T_H17 cell differentiation in vitro

(a) Flow cytometry of in vitro activated CFSE-labeled $CD4^+$ T cells for 72 h.

(b) Flow cytometry of $CD4^+$ T cells from control and *miR-21*$^{-/-}$ mice differentiated under T_H17(b) and T_H17(23) condition.

(c) Percentage of $IL17A^+$ T cells as in shown in (b) under T_H17(b) condition (n=4).

(d) Percentage of IL17A^{+} T cells as in shown in (b) under $T_H17(23)$ condition (n=4).

(e) Relative expression of miR-21 in CD4^{+} T cells from CD4-cre and CD4-cre *miR-21*$^{f/f}$ mice (n=4).

*P < 0.05 (unpaired t-test). Data are from one experiment representative of more than three independent experiments (mean and s. d. in c, d, e).

Supplementary Fig. 4

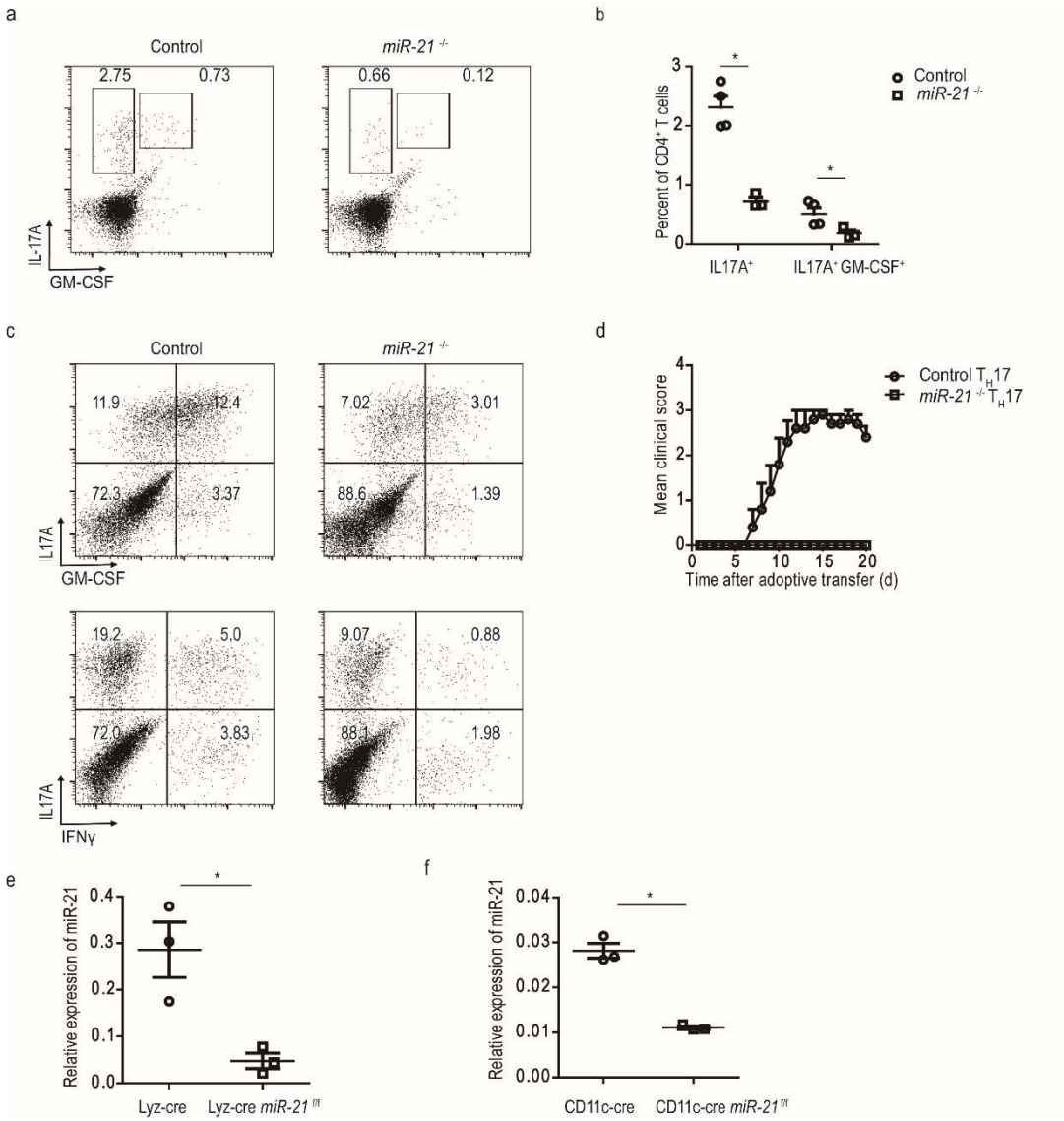

Supplementary Fig. 4 MiR-21$^{-/-}$ pathogenic T_H17 cannot transfer EAE disease to naïve recipients

(a) Flow cytometry of IL-17A and GM-CSF secretion by CD4$^+$ T cells isolated from splenocytes of control and *miR-21$^{-/-}$* mice immunized with MOG_{35-55} in CFA for 10 days (n=4).

(b) Percentage of IL17A$^+$ GM-CSF$^-$, IL17A$^+$ GM-CSF$^+$ cells as shown in (a).

(c) Flow cytometry of IL-17A and GM-CSF secretion (upper), IL-17A and IFN-

γ secretion (lower) by $CD4^+$ T cells from splenocytes (as in a) stimulated in vitro by MOG_{35-55} and IL-23 for 4 days (n = 4).

(d) EAE development of naïve C57 BL/6 mice transferred with pathogenic T_H17 cells (as in c) (n=6).

(e) Relative expression of miR-21 in in vitro derived macrophages from Lyz2-cre and Lyz2-cre *miR-21*$^{f/f}$ mice (n=4).

(f) Relative expression of miR-21 in in vitro derived FLT3L-DC cells from CD11c-cre and CD11c-cre *miR-21*$^{f/f}$ mice (n=4).

*P < 0.05 (unpaired t-test). Data are from one experiment representative of two independent experiments (mean and s. d. in b, e, f).

Supplementary Fig. 5

a

GO Term	P-Value
immune response	1.80E-06
glucose metabolic process	6.90E-06
monosaccharide metabolic process	1.10E-05
hexose metabolic process	1.10E-05
cell activation	1.50E-05
regulation of cell activation	2.20E-05
negative regulation of T cell activation	2.20E-05
negative regulation of immune system process	2.70E-05
generation of precursor metabolites and energy	3.20E-05

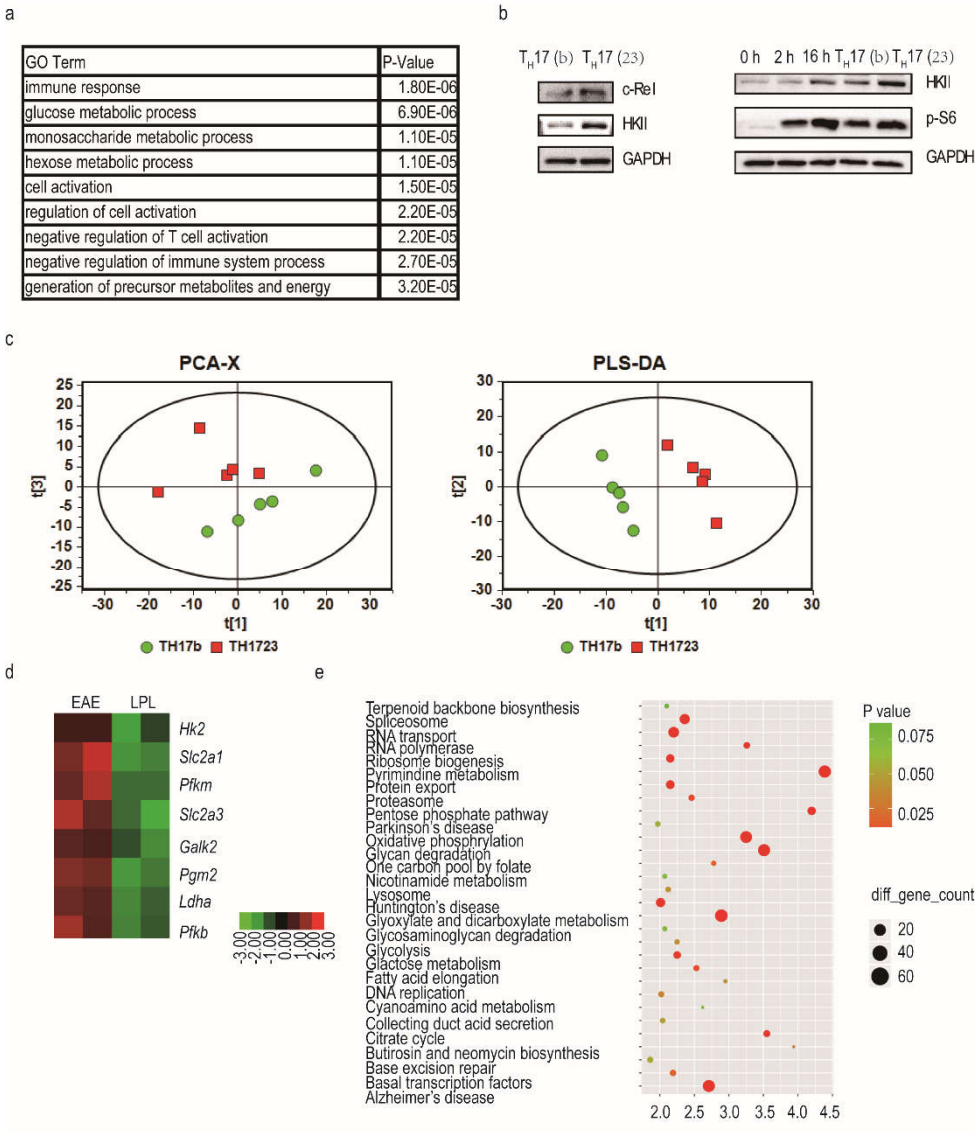

Supplementary Fig. 5 Pathogenic and non-pathogenic T_H17 cells have discrete metabolic states in vivo and in vitro

(a) GO pathway analysis by DAVID bioinformatics.

(b) Western blot analyses of c-Rel and HKII (left) in sorted T_H17(b) and T_H17(23) cells, HKII and p-S6 in $CD4^+$ T cells differentiated under indicated condition for 0 to 72h (right).

(c) PCA and PLS-OA analyses of the annotated metabolites from T_H17(b) and

$T_H17(23)$ cells.

(d) Heatmap of selected genes related to the glycolysis pathway from differentially expressed genes of homeostatic LPL and pathogenic EAE T_H17 cells, mRNA sequencing data was from ref[13].

(e) GO Pathway analyses of differentially expressed genes of LPL and EAE T_H17 cells, mRNA sequencing data was from ref[13].

Supplementary Fig. 6

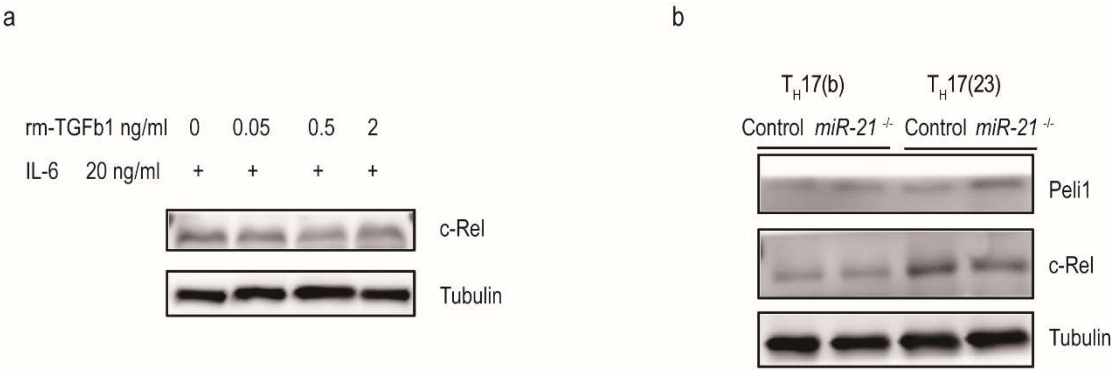

Supplementary Fig. 6 TGFb1 signaling inhibits c-Rel protein expression in T_H17(b) cells

(a) Western blot analyses of $CD4^+$ T cells differentiated under indicated condition for 72 h.

(b) Western blot analysis of Peli1 and c-Rel from T_H17 cells differentiated under indicated condition.

1. Littman DR, Rudensky AY. Th17 and regulatory T cells in mediating and restraining inflammation. *Cell* 2010, **140**(6)**:** 845-858.

2. Stockinger B, Omenetti S. The dichotomous nature of T helper 17 cells. *Nature reviews Immunology* 2017.

3. Ivanov, II, Atarashi K, Manel N, Brodie EL, Shima T, Karaoz U*, et al.* Induction of intestinal Th17 cells by segmented filamentous bacteria. *Cell* 2009, **139**(3)**:** 485-498.

4. Sano T, Huang W, Hall JA, Yang Y, Chen A, Gavzy SJ*, et al.* An IL-23R/IL-22 Circuit Regulates Epithelial Serum Amyloid A to Promote Local Effector Th17 Responses. *Cell* 2015, **163**(2)**:** 381-393.

5. Atarashi K, Tanoue T, Ando M, Kamada N, Nagano Y, Narushima S*, et al.* Th17 Cell Induction by Adhesion of Microbes to Intestinal Epithelial Cells. *Cell* 2015, **163**(2)**:** 367-380.

6. Zielinski CE, Mele F, Aschenbrenner D, Jarrossay D, Ronchi F, Gattorno M*, et al.* Pathogen-induced human TH17 cells produce IFN-gamma or IL-10 and are regulated by IL-1beta. *Nature* 2012, **484**(7395)**:** 514-518.

7. McGeachy MJ, Bak-Jensen KS, Chen Y, Tato CM, Blumenschein W, McClanahan T*, et al.* TGF-beta and IL-6 drive the production of IL-17 and IL-10 by T cells and restrain T(H)-17 cell-mediated pathology. *Nature immunology* 2007, **8**(12)**:** 1390-1397.

8. Ghoreschi K, Laurence A, Yang XP, Tato CM, McGeachy MJ, Konkel JE*, et al.* Generation of pathogenic T(H)17 cells in the absence of TGF-beta signalling. *Nature* 2010, **467**(7318)**:** 967-971.

9. El-Behi M, Ciric B, Dai H, Yan Y, Cullimore M, Safavi F*, et al.* The encephalitogenicity of T(H)17 cells is dependent on IL-1- and IL-23-induced production of the cytokine GM-CSF. *Nature immunology* 2011, **12**(6)**:** 568-575.

10. Codarri L, Gyulveszi G, Tosevski V, Hesske L, Fontana A, Magnenat L*, et al.* RORgammat drives production of the cytokine GM-CSF in helper T cells, which is essential for the effector phase of autoimmune neuroinflammation. *Nature immunology* 2011, **12**(6)**:** 560-567.

11. Wu C, Yosef N, Thalhamer T, Zhu C, Xiao S, Kishi Y*, et al.* Induction of pathogenic TH17 cells by inducible salt-sensing kinase SGK1. *Nature* 2013, **496**(7446)**:** 513-517.

12. Kleinewietfeld M, Manzel A, Titze J, Kvakan H, Yosef N, Linker RA*, et al.* Sodium chloride drives autoimmune disease by the induction of pathogenic TH17 cells. *Nature* 2013, **496**(7446)**:** 518-522.

13. Gaublomme JT, Yosef N, Lee Y, Gertner RS, Yang LV, Wu C*, et al.* Single-Cell Genomics Unveils Critical Regulators of Th17 Cell Pathogenicity. *Cell* 2015, **163**(6)**:** 1400-1412.

14. Wang C, Yosef N, Gaublomme J, Wu C, Lee Y, Clish CB*, et al.* CD5L/AIM Regulates Lipid Biosynthesis and Restrains Th17 Cell Pathogenicity. *Cell* 2015, **163**(6)**:** 1413-1427.

15. Buck MD, O'Sullivan D, Pearce EL. T cell metabolism drives immunity. *The Journal of experimental medicine* 2015, **212**(9)**:** 1345-1360.

16. Man K, Kallies A. Synchronizing transcriptional control of T cell metabolism and function. *Nature reviews Immunology* 2015, **15**(9)**:** 574-584.

17. Pollizzi KN, Powell JD. Integrating canonical and metabolic signalling programmes in the regulation of T cell responses. *Nature reviews Immunology* 2014, **14**(7)**:** 435-446.

18. Wang R, Dillon CP, Shi LZ, Milasta S, Carter R, Finkelstein D*, et al.* The transcription factor

Myc controls metabolic reprogramming upon T lymphocyte activation. *Immunity* 2011, **35**(6)**:** 871-882.

19. Verbist KC, Guy CS, Milasta S, Liedmann S, Kaminski MM, Wang R*, et al.* Metabolic maintenance of cell asymmetry following division in activated T lymphocytes. *Nature* 2016, **532**(7599)**:** 389-393.

20. Boothby M, Rickert RC. Metabolic Regulation of the Immune Humoral Response. *Immunity* 2017, **46**(5)**:** 743-755.

21. Heise N, De Silva NS, Silva K, Carette A, Simonetti G, Pasparakis M*, et al.* Germinal center B cell maintenance and differentiation are controlled by distinct NF-kappaB transcription factor subunits. *The Journal of experimental medicine* 2014, **211**(10)**:** 2103-2118.

22. Shi LZ, Wang R, Huang G, Vogel P, Neale G, Green DR*, et al.* HIF1alpha-dependent glycolytic pathway orchestrates a metabolic checkpoint for the differentiation of TH17 and Treg cells. *The Journal of experimental medicine* 2011, **208**(7)**:** 1367-1376.

23. Wilhelm K, Happel K, Eelen G, Schoors S, Oellerich MF, Lim R*, et al.* FOXO1 couples metabolic activity and growth state in the vascular endothelium. *Nature* 2016, **529**(7585)**:** 216-220.

24. Angelin A, Gil-de-Gomez L, Dahiya S, Jiao J, Guo L, Levine MH*, et al.* Foxp3 Reprograms T Cell Metabolism to Function in Low-Glucose, High-Lactate Environments. *Cell metabolism* 2017.

25. Ho PC, Bihuniak JD, Macintyre AN, Staron M, Liu X, Amezquita R*, et al.* Phosphoenolpyruvate Is a Metabolic Checkpoint of Anti-tumor T Cell Responses. *Cell* 2015, **162**(6)**:** 1217-1228.

26. Chang CH, Qiu J, O'Sullivan D, Buck MD, Noguchi T, Curtis JD*, et al.* Metabolic Competition in the Tumor Microenvironment Is a Driver of Cancer Progression. *Cell* 2015, **162**(6)**:** 1229-1241.

27. Mehta A, Baltimore D. MicroRNAs as regulatory elements in immune system logic. *Nature reviews Immunology* 2016, **16**(5)**:** 279-294.

28. Boldin MP, Taganov KD, Rao DS, Yang L, Zhao JL, Kalwani M*, et al.* miR-146a is a significant brake on autoimmunity, myeloproliferation, and cancer in mice. *The Journal of experimental medicine* 2011, **208**(6)**:** 1189-1201.

29. Rodriguez A, Vigorito E, Clare S, Warren MV, Couttet P, Soond DR*, et al.* Requirement of bic/microRNA-155 for normal immune function. *Science (New York, NY)* 2007, **316**(5824)**:** 608-611.

30. Thai TH, Calado DP, Casola S, Ansel KM, Xiao C, Xue Y*, et al.* Regulation of the germinal center response by microRNA-155. *Science (New York, NY)* 2007, **316**(5824)**:** 604-608.

31. O'Connell RM, Kahn D, Gibson WS, Round JL, Scholz RL, Chaudhuri AA*, et al.* MicroRNA-155 promotes autoimmune inflammation by enhancing inflammatory T cell development. *Immunity* 2010, **33**(4)**:** 607-619.

32. Escobar TM, Kanellopoulou C, Kugler DG, Kilaru G, Nguyen CK, Nagarajan V*, et al.* miR-155 activates cytokine gene expression in Th17 cells by regulating the DNA-binding protein Jarid2 to relieve polycomb-mediated repression. *Immunity* 2014, **40**(6)**:** 865-879.

33. Hu R, Kagele DA, Huffaker TB, Runtsch MC, Alexander M, Liu J*, et al.* miR-155 promotes T follicular helper cell accumulation during chronic, low-grade inflammation. *Immunity* 2014, **41**(4)**:** 605-619.

34. Ichiyama K, Gonzalez-Martin A, Kim BS, Jin HY, Jin W, Xu W*, et al.* The MicroRNA-183-96-182 Cluster Promotes T Helper 17 Cell Pathogenicity by Negatively Regulating Transcription Factor Foxo1 Expression. *Immunity* 2016, **44**(6)**:** 1284-1298.

35. Buenrostro JD, Giresi PG, Zaba LC, Chang HY, Greenleaf WJ. Transposition of native chromatin for fast and sensitive epigenomic profiling of open chromatin, DNA-binding proteins and nucleosome position. *Nature methods* 2013, **10**(12)**:** 1213-1218.

36. van der Veeken J, Gonzalez AJ, Cho H, Arvey A, Hemmers S, Leslie CS*, et al.* Memory of Inflammation in Regulatory T Cells. *Cell* 2016, **166**(4)**:** 977-990.

37. Ceribelli M, Hou ZE, Kelly PN, Huang DW, Wright G, Ganapathi K*, et al.* A Druggable TCF4- and BRD4-Dependent Transcriptional Network Sustains Malignancy in Blastic Plasmacytoid Dendritic Cell Neoplasm. *Cancer cell* 2016, **30**(5)**:** 764-778.

38. Philip M, Fairchild L, Sun L, Horste EL, Camara S, Shakiba M*, et al.* Chromatin states define tumour-specific T cell dysfunction and reprogramming. *Nature* 2017, **545**(7655)**:** 452-456.

39. Murugaiyan G, da Cunha AP, Ajay AK, Joller N, Garo LP, Kumaradevan S*, et al.* MicroRNA-21 promotes Th17 differentiation and mediates experimental autoimmune encephalomyelitis. *The Journal of clinical investigation* 2015, **125**(3)**:** 1069-1080.

40. Pua HH, Steiner DF, Patel S, Gonzalez JR, Ortiz-Carpena JF, Kageyama R*, et al.* MicroRNAs 24 and 27 Suppress Allergic Inflammation and Target a Network of Regulators of T Helper 2 Cell-Associated Cytokine Production. *Immunity* 2016, **44**(4)**:** 821-832.

41. Pan W, Zhu S, Dai D, Liu Z, Li D, Li B*, et al.* MiR-125a targets effector programs to stabilize Treg-mediated immune homeostasis. *Nature communications* 2015, **6:** 7096.

42. Cho S, Wu CJ, Yasuda T, Cruz LO, Khan AA, Lin LL*, et al.* miR-23 approximately 27 approximately 24 clusters control effector T cell differentiation and function. *The Journal of experimental medicine* 2016, **213**(2)**:** 235-249.

43. Zhu S, Pan W, Song X, Liu Y, Shao X, Tang Y*, et al.* The microRNA miR-23b suppresses IL-17-associated autoimmune inflammation by targeting TAB2, TAB3 and IKK-alpha. *Nature medicine* 2012, **18**(7)**:** 1077-1086.

44. Huang da W, Sherman BT, Lempicki RA. Systematic and integrative analysis of large gene lists using DAVID bioinformatics resources. *Nature protocols* 2009, **4**(1)**:** 44-57.

45. Ciofani M, Madar A, Galan C, Sellars M, Mace K, Pauli F*, et al.* A validated regulatory network for Th17 cell specification. *Cell* 2012, **151**(2)**:** 289-303.

46. Loeb GB, Khan AA, Canner D, Hiatt JB, Shendure J, Darnell RB*, et al.* Transcriptome-wide miR-155 binding map reveals widespread noncanonical microRNA targeting. *Molecular cell* 2012, **48**(5)**:** 760-770.

47. Chang M, Jin W, Chang JH, Xiao Y, Brittain GC, Yu J*, et al.* The ubiquitin ligase Peli1 negatively regulates T cell activation and prevents autoimmunity. *Nature immunology* 2011, **12**(10)**:** 1002-1009.

48. Ruan Q, Kameswaran V, Zhang Y, Zheng S, Sun J, Wang J*, et al.* The Th17 immune response is controlled by the Rel-RORgamma-RORgamma T transcriptional axis. *The Journal of experimental medicine* 2011, **208**(11)**:** 2321-2333.

49. Sellick CA, Hansen R, Stephens GM, Goodacre R, Dickson AJ. Metabolite extraction from suspension-cultured mammalian cells for global metabolite profiling. *Nature protocols* 2011, **6**(8)**:** 1241-1249.

50. Jin H, Qiao F, Chen L, Lu C, Xu L, Gao X. Serum metabolomic signatures of lymph node metastasis of esophageal squamous cell carcinoma. *Journal of proteome research* 2014, **13**(9)**:** 4091-4103.